

Random matrices, spectral measures, and composite media

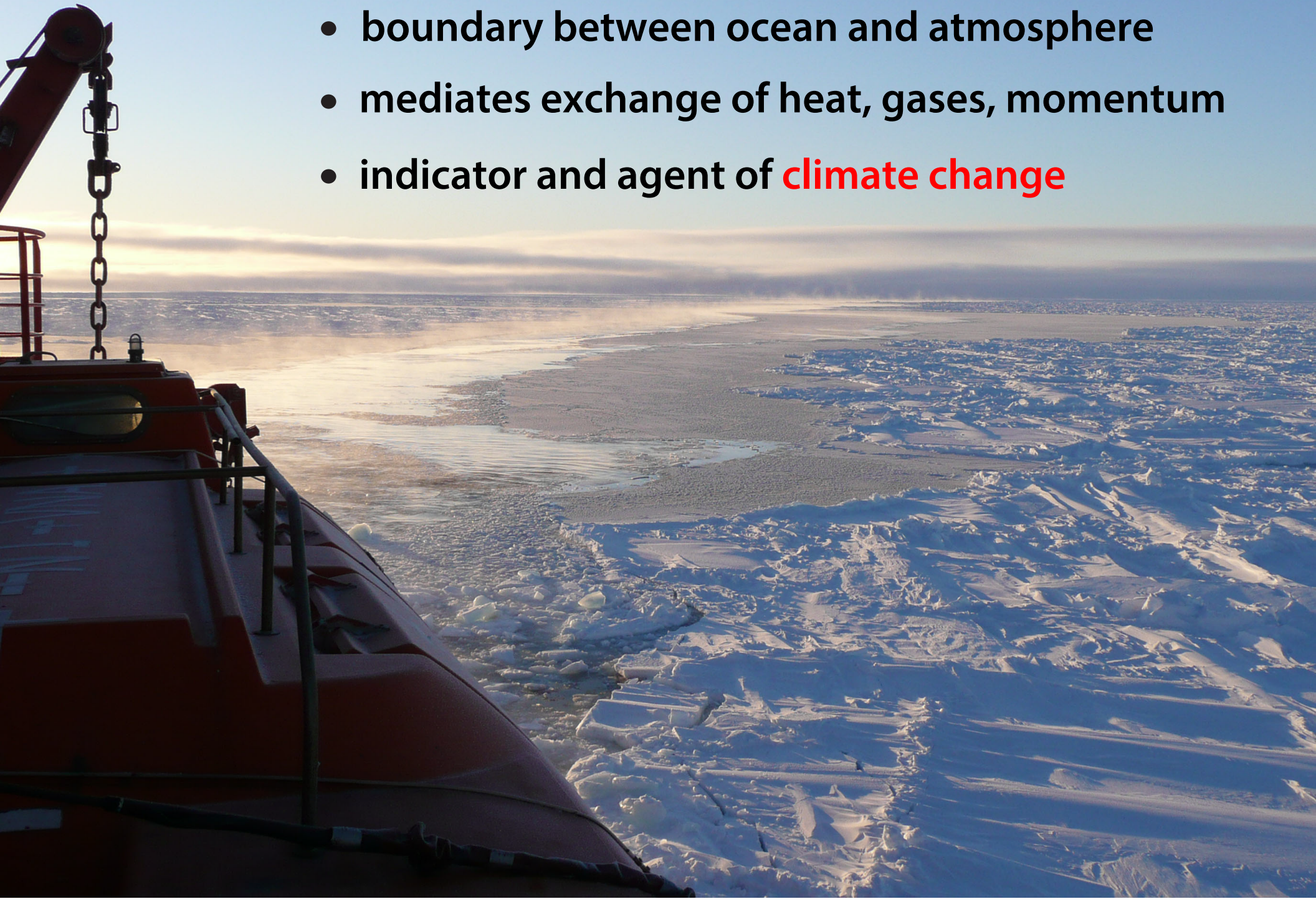
N. Benjamin Murphy and Kenneth M. Golden, Department of Mathematics, University of Utah



*SIAM Conference on Mathematics of Materials
MS1: Stochastic Homogenization
Philadelphia, 9 June 2013*

SEA ICE covers 7 - 10% of earth's ocean surface

- boundary between ocean and atmosphere
- mediates exchange of heat, gases, momentum
- indicator and agent of **climate change**



polar ice caps critical to global climate in reflecting incoming solar radiation



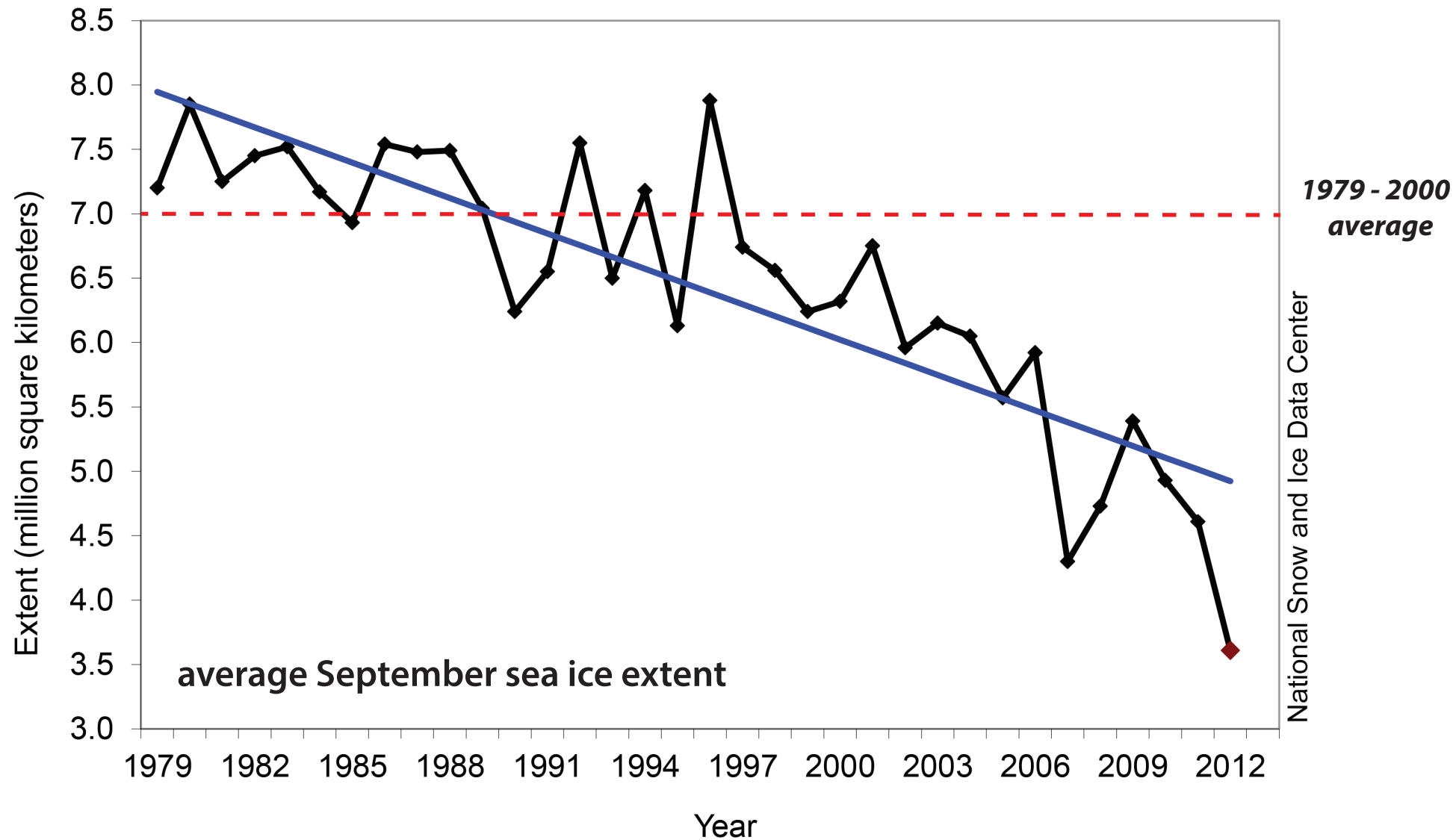
white snow and ice
reflect



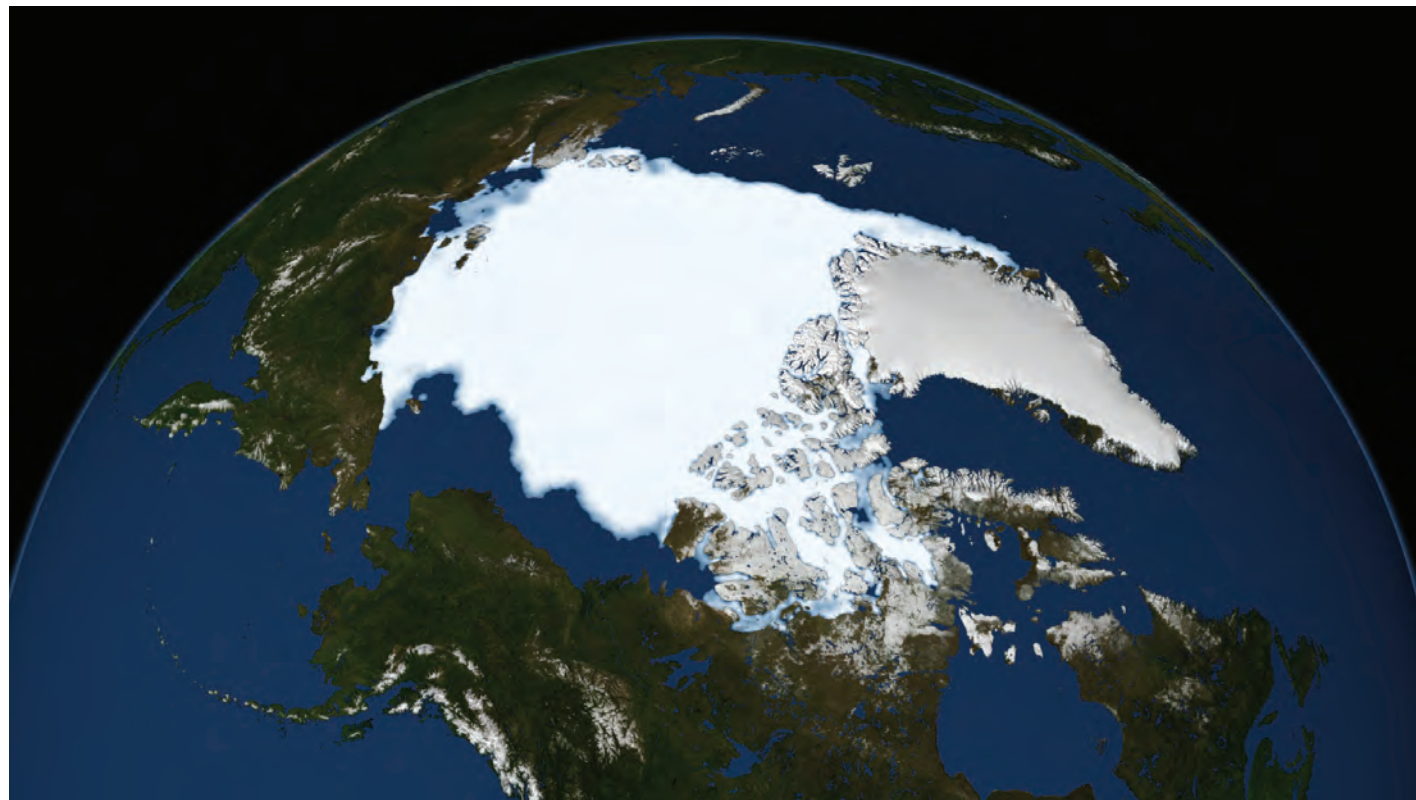
dark water and land
absorb

$$\text{albedo } \alpha = \frac{\text{reflected sunlight}}{\text{incident sunlight}}$$

the summer Arctic sea ice pack is melting

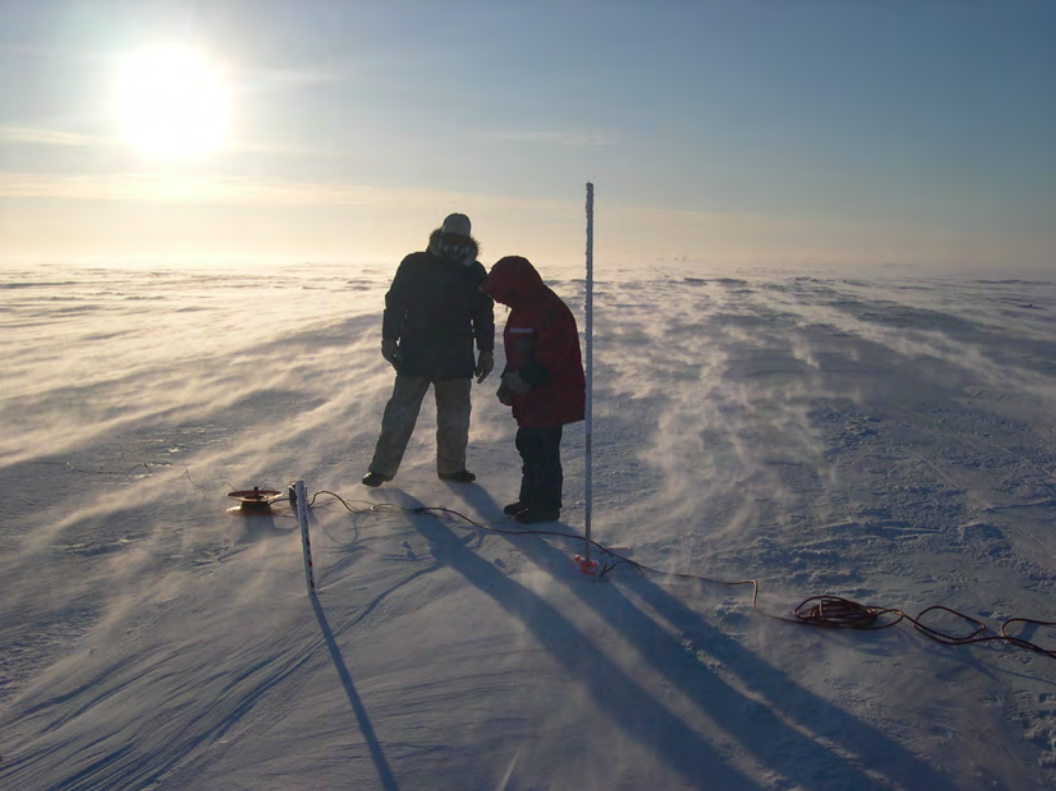


21 September 1979



13 September 2012

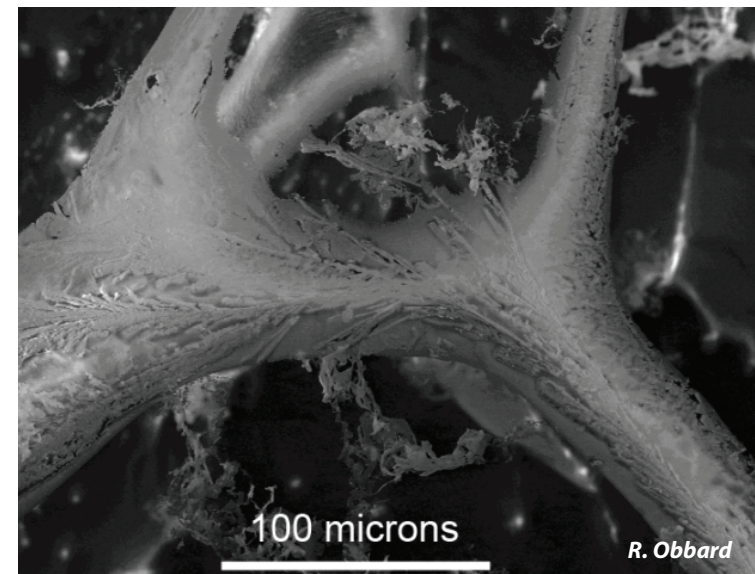




*sea ice may appear to be a
barren, impermeable cap ...*



brine inclusions in sea ice (mm)



micro - brine channel (SEM)

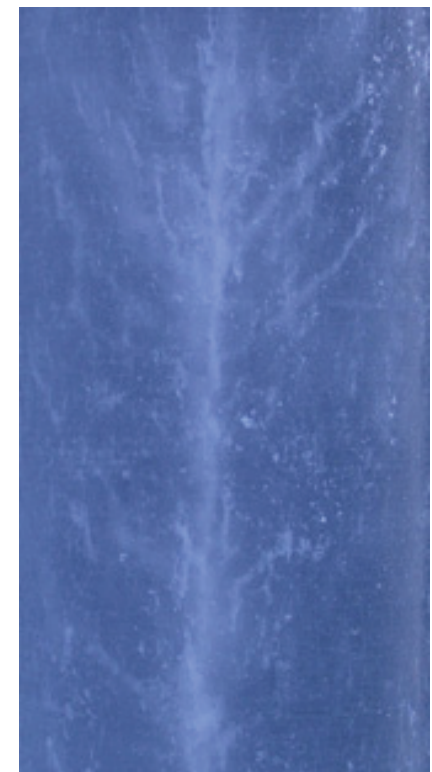
***sea ice is a
porous composite***

pure ice with brine, air, and salt inclusions

brine channels (cm)



horizontal section



vertical section

fluid flow through the porous microstructure of sea ice governs key processes in polar climate and ecosystems:

evolution of Arctic melt ponds and sea ice albedo



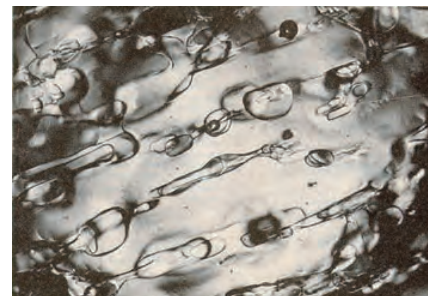
nutrient flux for algal communities



- drainage of brine and melt water
- ocean-ice-air exchanges of heat, CO₂



linkage of scales



What is this talk about? (+ preview of afternoon lecture)

Using the mathematics of composite materials and statistical physics to study sea ice structures and processes ... to improve projections of climate change.

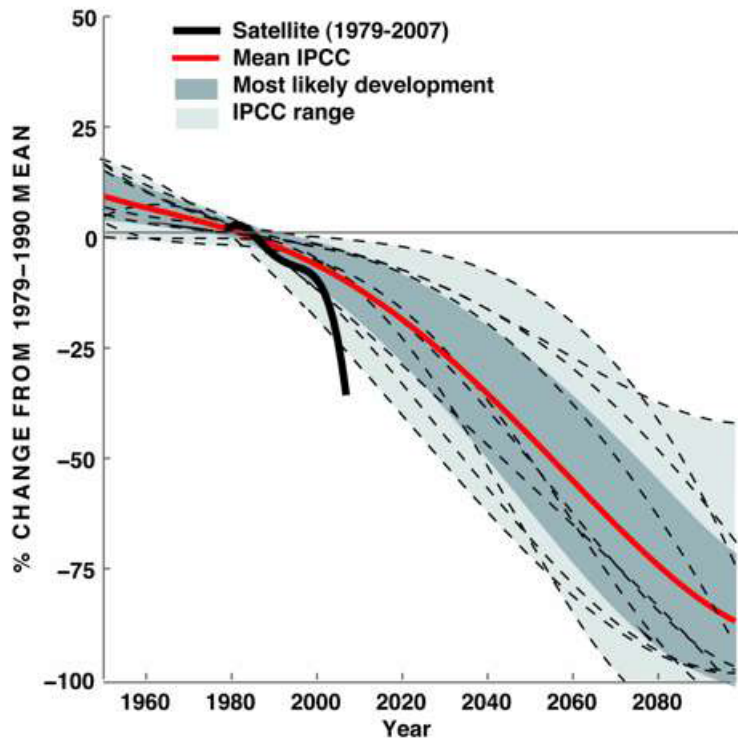
- 1. ***Fluid flow through sea ice*** - percolation, flow in porous media
- 2. ***Arctic and Antarctic experiments*** on fluid and electrical transport
- 3. ***Fractal structure*** - floe and melt pond configurations
- 4. ***Multiscale Homogenization*** - spectral upscaling, random matrices

critical behavior linkage of scales

.... and to suggest a path forward for more rigorously and efficiently representing sea ice in climate models.

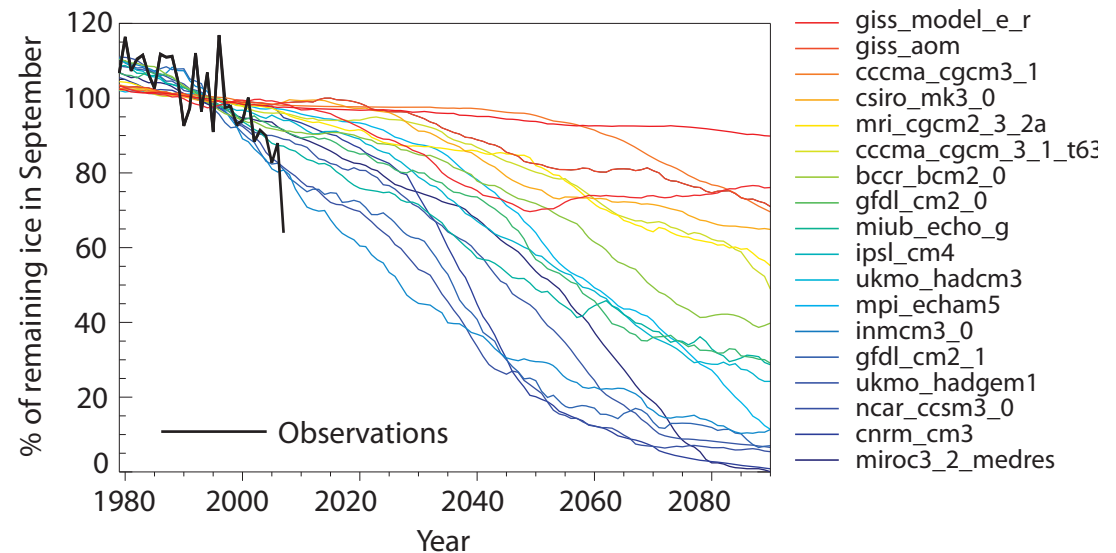
Intergovernmental Panel on Climate Change (IPCC) 2007 projections

*observed decline in summer Arctic sea ice
outpacing global climate models*



Arctic sea ice loss compared to IPCC models

September 2007



March 2009

Boé, Hall, Qu 2009

sea ice microphysics

fluid transport

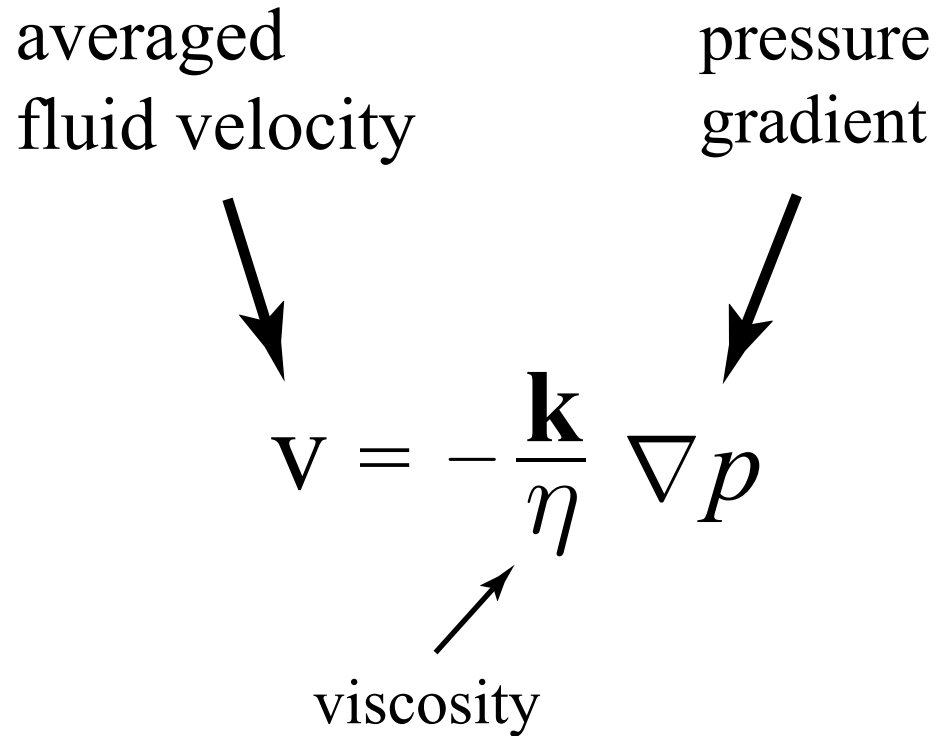
Darcy's Law for slow viscous flow in a porous medium

averaged
fluid velocity

pressure
gradient

$$\mathbf{v} = -\frac{\mathbf{k}}{\eta} \nabla p$$

viscosity

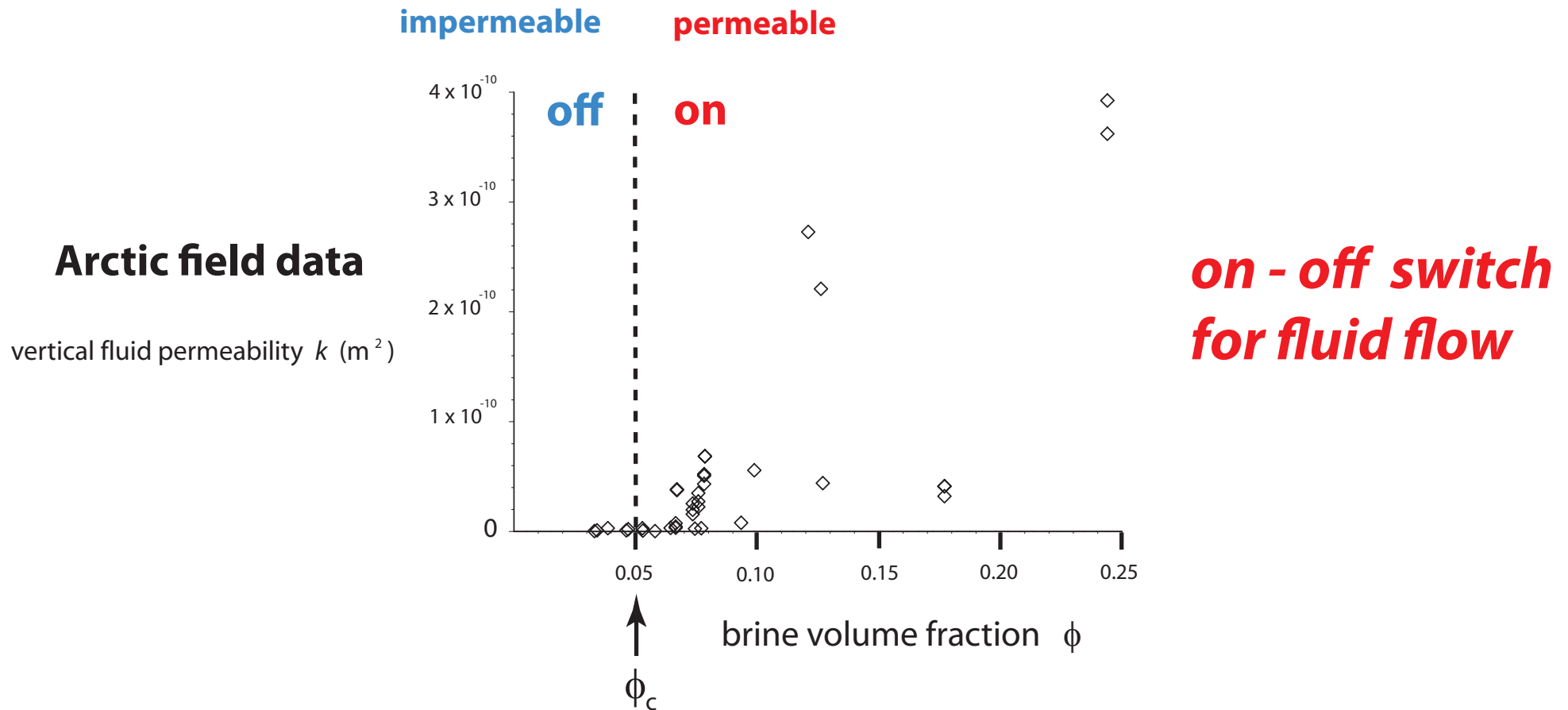
The diagram shows the equation $\mathbf{v} = -\frac{\mathbf{k}}{\eta} \nabla p$ centered on the slide. Three labels with arrows point to parts of the equation: 'averaged fluid velocity' points to \mathbf{v} , 'pressure gradient' points to ∇p , and 'viscosity' points to η .

\mathbf{k} = fluid permeability tensor

example of *homogenization*

mathematics for analyzing effective behavior of heterogeneous systems

Critical behavior of fluid transport in sea ice



critical brine volume fraction $\phi_c \approx 5\%$ \longleftrightarrow $T_c \approx -5^\circ \text{C}$, $S \approx 5 \text{ ppt}$

RULE OF FIVES

Golden, Ackley, Lytle *Science* 1998

Golden, Eicken, Heaton, Miner, Pringle, Zhu, *Geophys. Res. Lett.* 2007

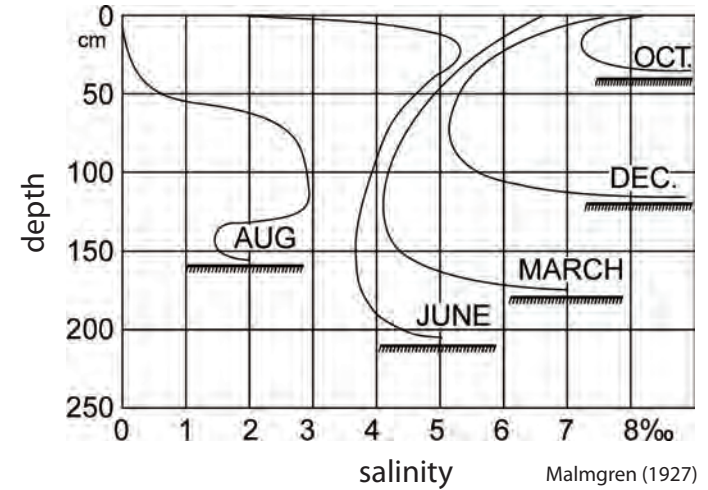
Pringle, Miner, Eicken, Golden *J. Geophys. Res.* 2009

rule of fives constrains:

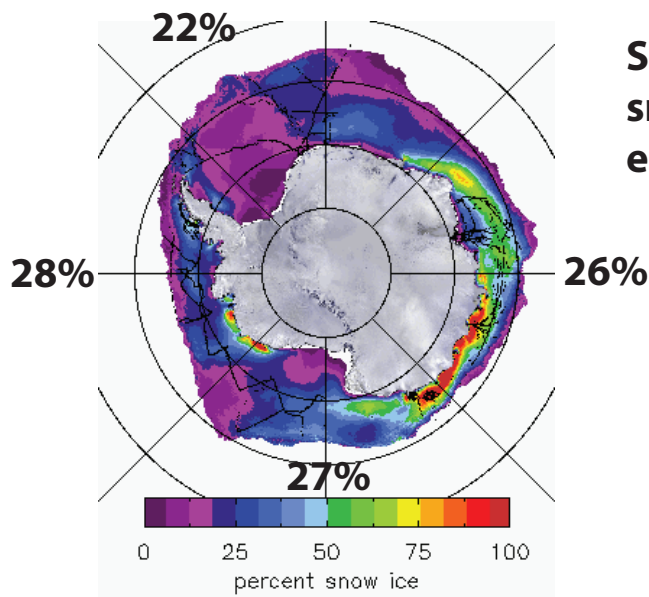
Antarctic surface flooding and snow-ice formation



evolution of salinity profiles



currently assumed constant in climate models



September
snow-ice
estimates

Antarctic snow-to-ice conversion from passive microwave imagery

T. Maksym and T. Markus, 2008

convection - enhanced thermal conductivity

Lytle and Ackley, 1996

Trodahl, et. al., 2000, 2001

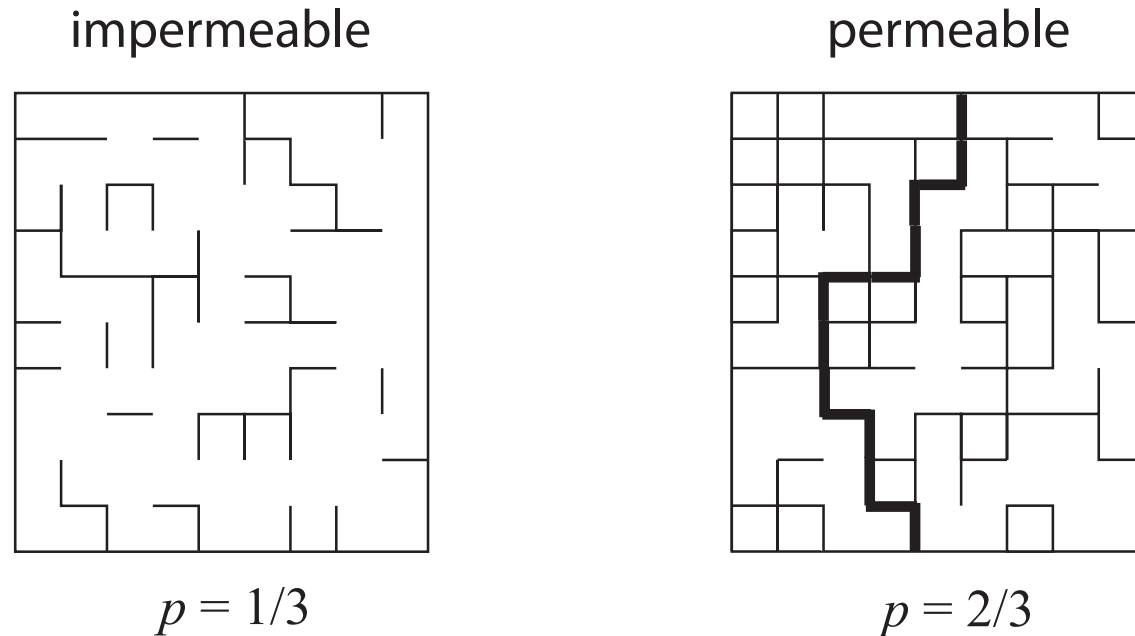
Wang, Zhu, Golden, 2012



**theoretical models explaining the
rule of fives and fluid flow properties**

percolation theory

mathematical theory of connectedness



bond \longrightarrow *open* with probability p
closed with probability $1-p$

percolation threshold

$$p_c = 1/2 \quad \text{for } d = 2$$

first appearance of infinite cluster

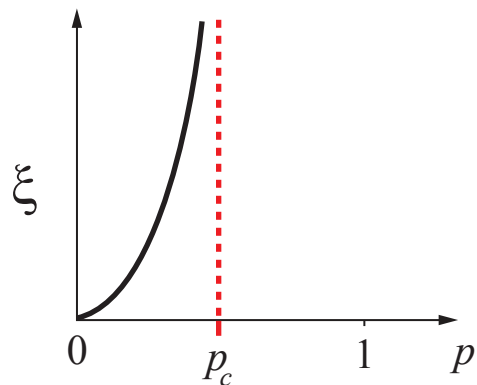
“tipping point” for connectivity

order parameters in percolation theory

geometry

correlation length

characteristic scale
of connectedness

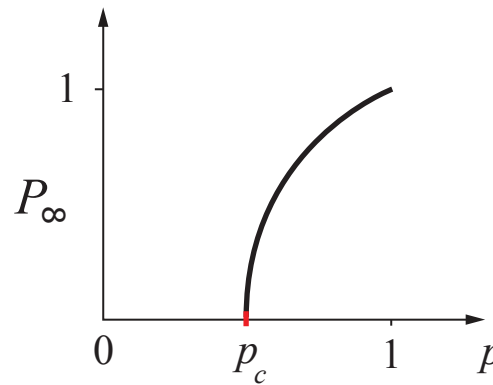


$$\xi(p) \sim |p - p_c|^{-\nu}$$

$$p \rightarrow p_c$$

infinite cluster density

probability the origin
belongs to infinite cluster

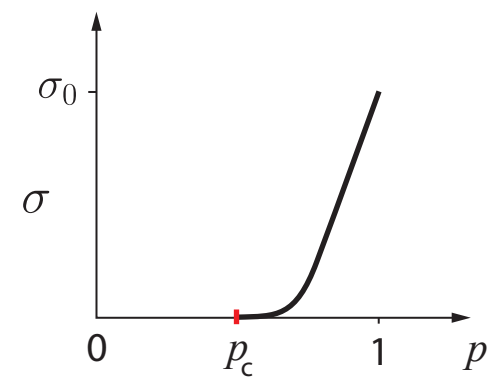


$$P_\infty(p) \sim (p - p_c)^\beta$$

$$p \rightarrow p_c^+$$

transport

effective conductivity
or fluid permeability



$$\sigma(p) \sim \sigma_0 (p - p_c)^t$$

$$p \rightarrow p_c^+$$

UNIVERSAL critical exponents for lattices -- depend only on dimension

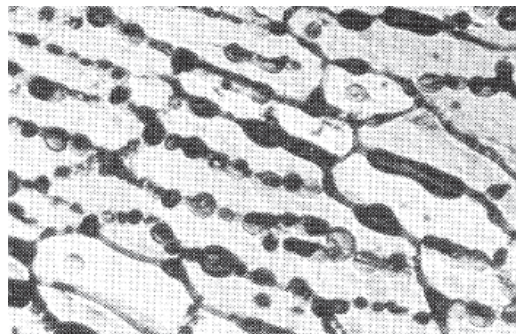
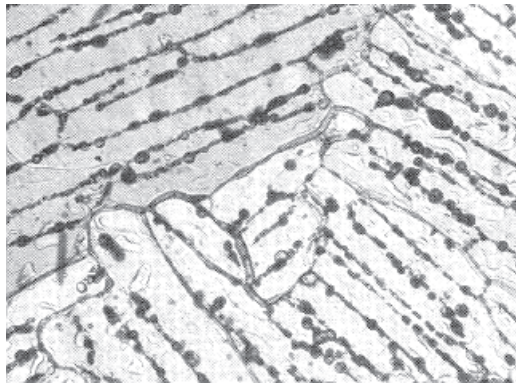
($1 \leq t \leq 2$, Golden, *Phys. Rev. Lett.* 1990 ; *Comm. Math. Phys.* 1992)

non-universal behavior in continuum

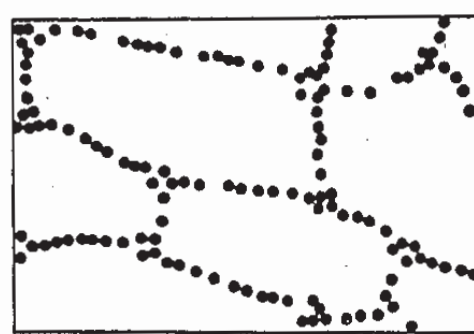
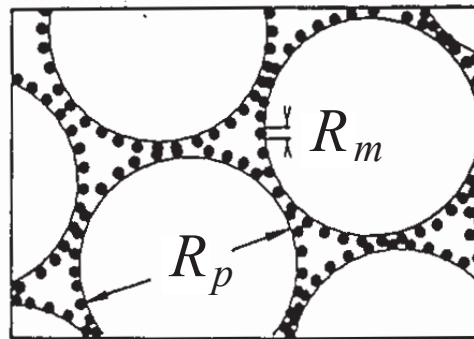
Continuum percolation model for stealthy materials applied to sea ice microstructure explains **Rule of Fives** and Antarctic data on **ice production** and **algal growth**

$$\phi_c \approx 5 \%$$

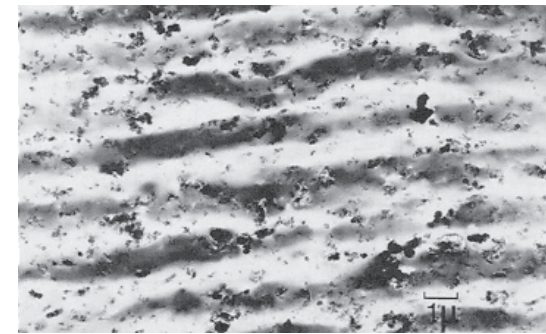
Golden, Ackley, Lytle, *Science*, 1998



sea ice



compressed
powder



radar absorbing
composite

sea ice is radar absorbing



***rigorous bounds
percolation theory
hierarchical model
network model***

field data

X-ray tomography for
brine inclusions

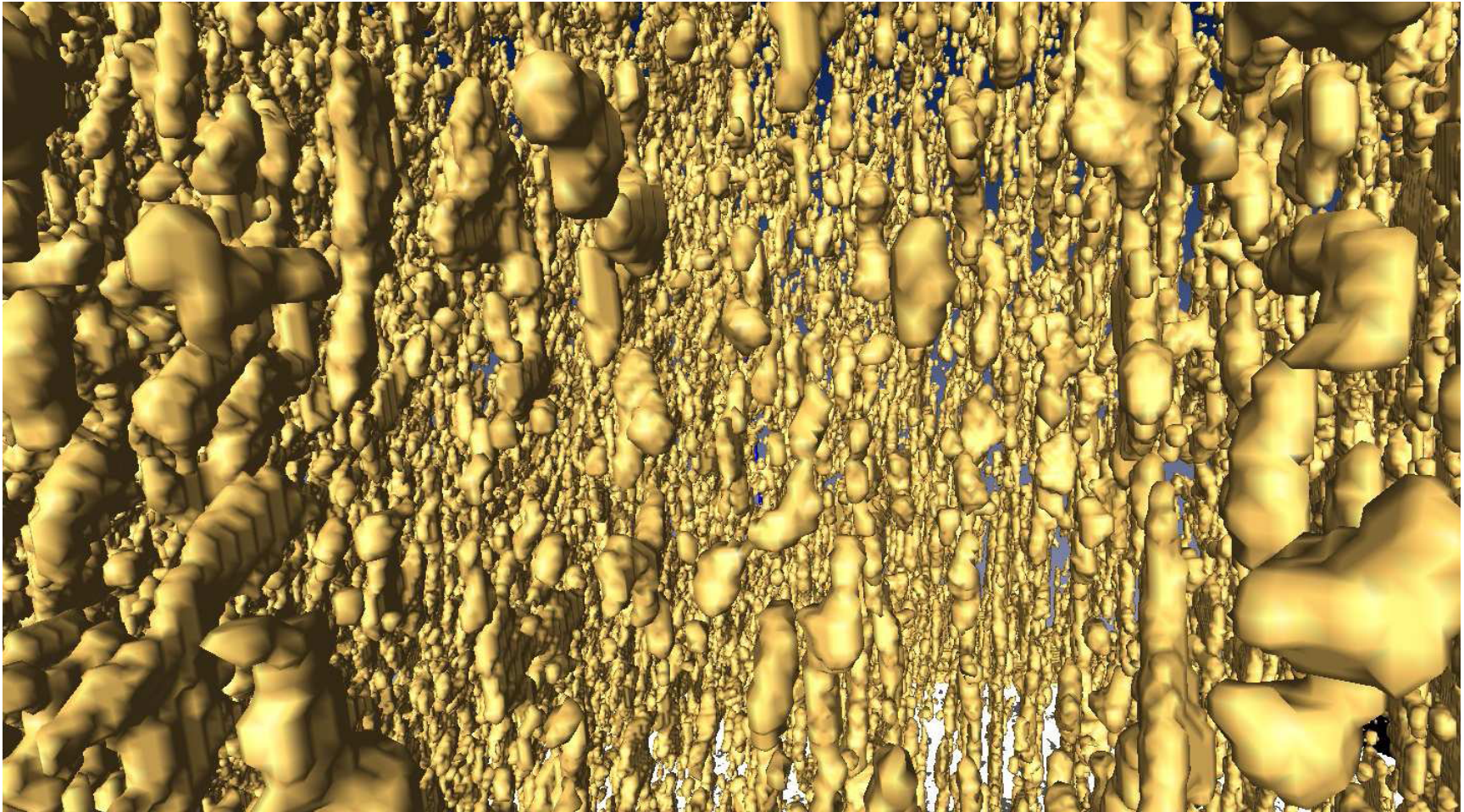
***unprecedented look
at thermal evolution
of brine phase and
its connectivity***

micro-scale
controls
macro-scale
processes

A unified approach to understanding permeability in sea ice • Solving the mystery of
booming sand dunes • Entering into the “greenhouse century”: A case study from Switzerland

X-ray computed tomography of brine inclusions in sea ice

~ 1 cm across

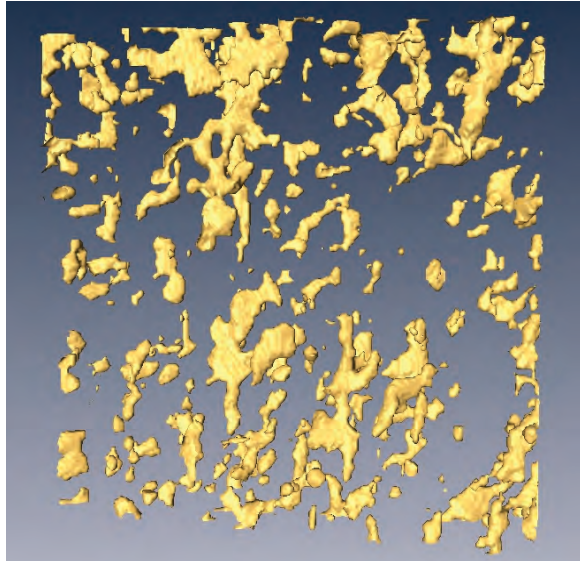


brine volume fraction $\phi = 5.7 \%$ $T = -8^{\circ}\text{C}$

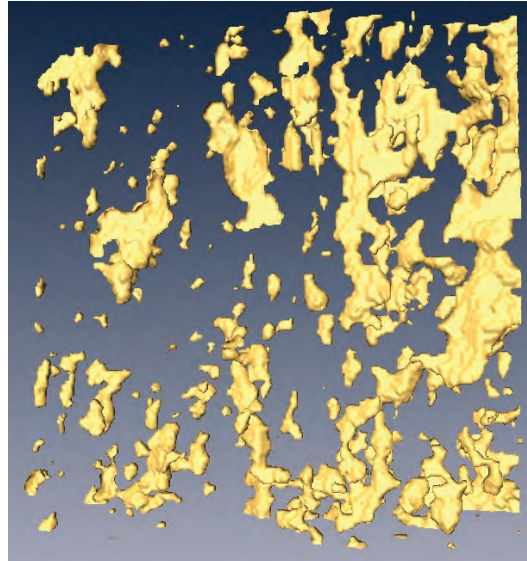
Golden, Eicken, Heaton, Miner, Pringle, Zhu, *Geophys. Res. Lett.* 2007

brine connectivity (over cm scale)

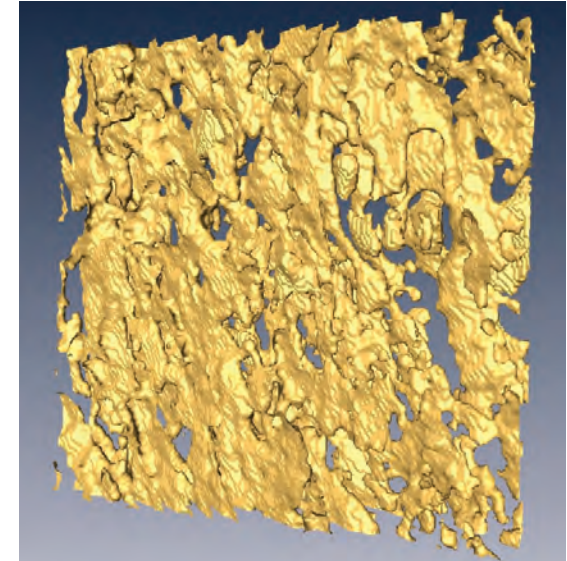
8 x 8 x 2 mm



-15 °C, $\phi = 0.033$



-6 °C, $\phi = 0.075$



-3 °C, $\phi = 0.143$

X-ray tomography confirms percolation threshold

3-D images
pores and throats



3-D graph
nodes and edges

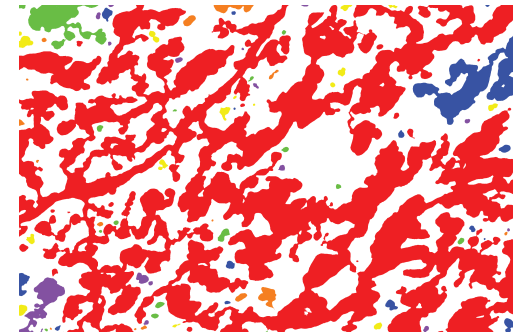
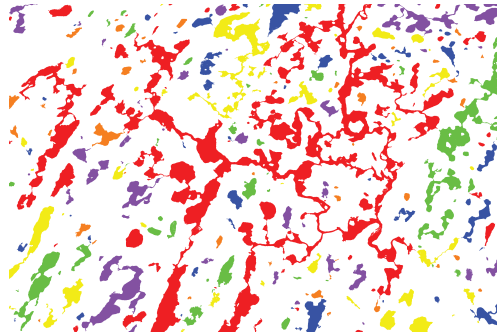
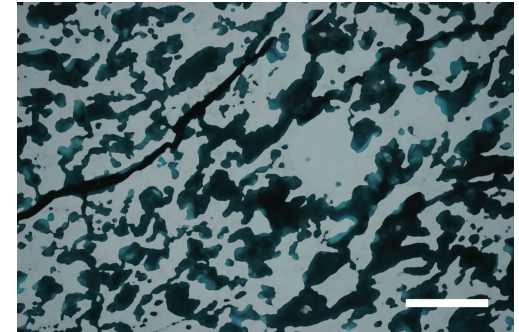
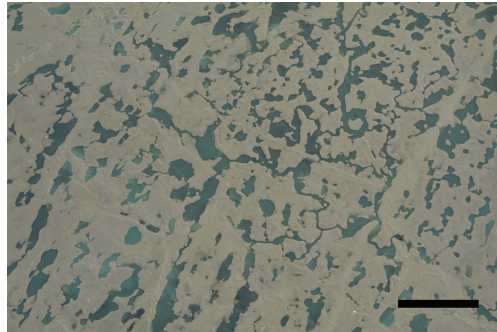
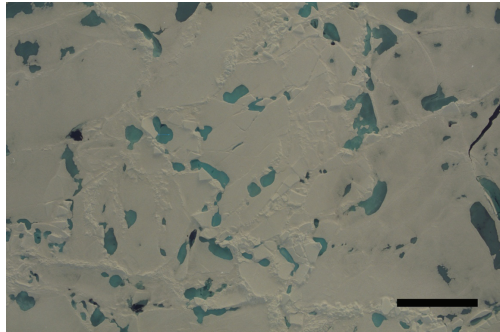
analyze graph connectivity as function of temperature and sample size

- ***use finite size scaling techniques to confirm rule of fives***
- ***order parameter data from a natural material***

melt ponds on the surface of Arctic sea ice



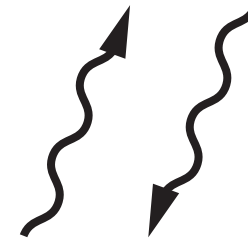
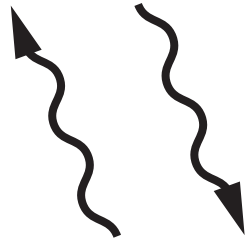
***small simple ponds coalesce to form
large connected structures with complex boundaries***



melt pond percolation

multiscale homogenization

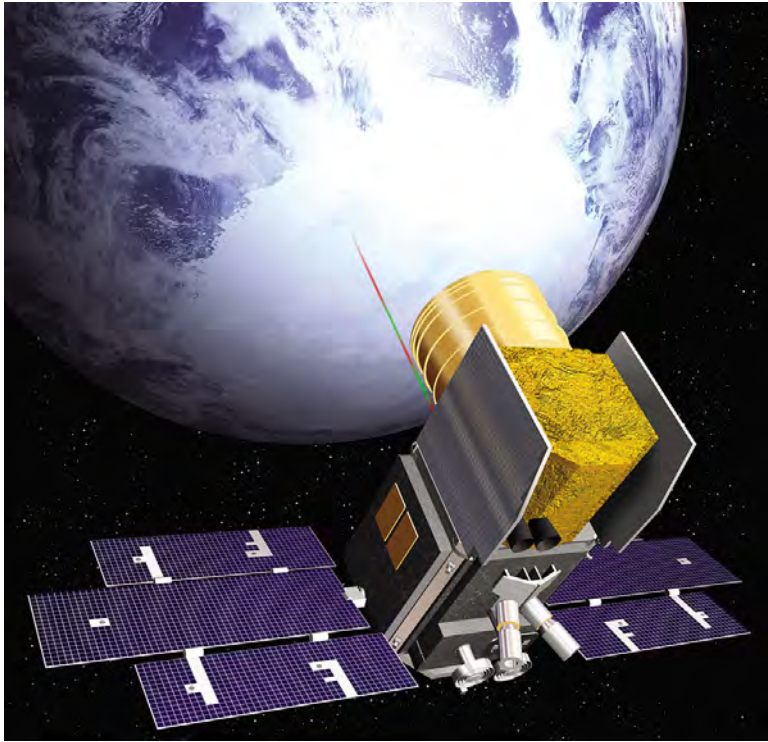
Remote sensing of sea ice



Recover sea ice
properties from
electromagnetic
(EM) data



INVERSE
PROBLEM



NASA's Ice, Cloud and Land Elevation Satellite (ICESat)



The Worbot - a low frequency EM induction instrument for measuring sea ice thickness

The key parameter in modeling the response of sea ice to an EM field is its

*complex permittivity or dielectric constant ϵ^**

which depends strongly on the brine microstructure

*e.g., interpretation of EM thickness data depends on knowledge of ϵ^**

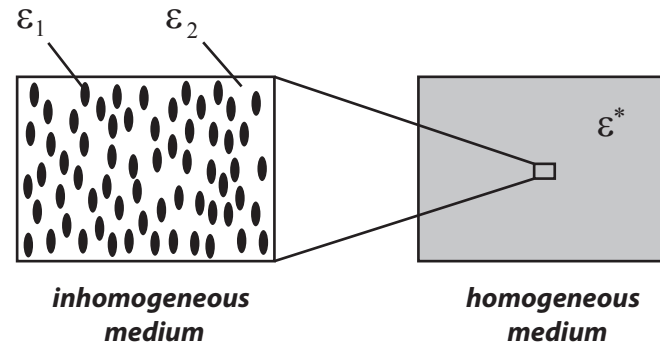
ocean swells propagating through a vast field of pancake ice

HOMOGENIZATION: long wave sees an effective medium, not individual floes



Theory of Effective Electromagnetic Behavior of Composites

analytic continuation method



Forward Homogenization Bergman (1978), Milton (1979), Golden and Papanicolaou (1983)

composite geometry
(spectral measure μ) \longrightarrow ϵ^*

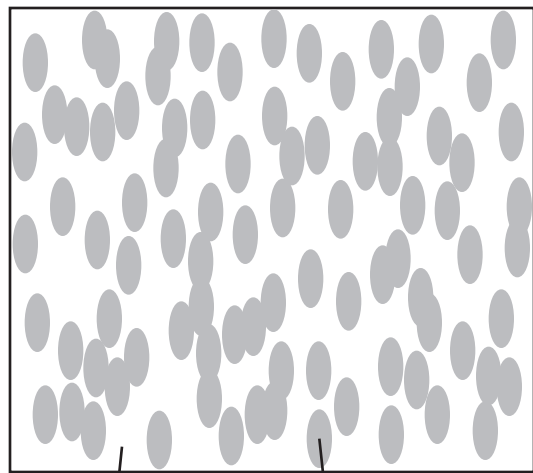
integral representations, rigorous bounds, approximations, etc.

Inverse Homogenization Cherkaev and Golden (1998), Day and Thorpe (1999), Cherkaev (2001)
(McPhedran, McKenzie, and Milton, 1982)

ϵ^* \longrightarrow **composite geometry**
(spectral measure μ)

recover brine volume fraction, connectivity, etc.

Effective complex permittivity of a two phase composite in the quasistatic (long wavelength) limit



ϵ_1

ϵ_2



ϵ^*

$$D = \epsilon E$$

$$\nabla \cdot D = 0$$

$$\nabla \times E = 0$$

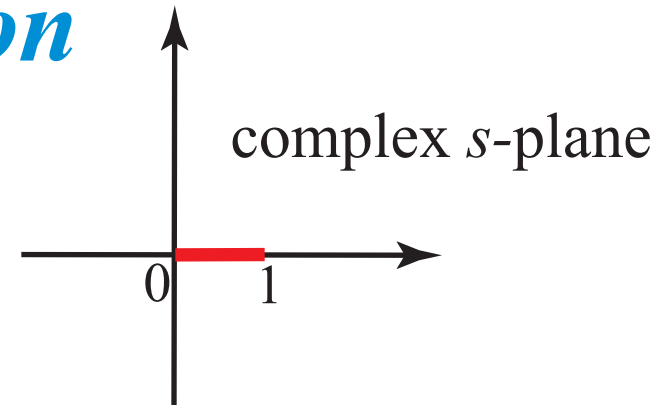
$$\langle D \rangle = \epsilon^* \langle E \rangle$$

p_1, p_2 = volume fractions of
the components

$$\epsilon^* = \epsilon^* \left(\frac{\epsilon_1}{\epsilon_2}, \text{ composite geometry } \right)$$

Stieltjes integral representation

$$F(s) = 1 - \frac{\epsilon^*}{\epsilon_2}, \quad s = \frac{1}{1 - \epsilon_1 / \epsilon_2}$$



$$F(s) = \int_0^1 \frac{d\mu(z)}{s - z}, \quad \mu$$

- spectral measure of self adjoint operator $\Gamma\chi$
- mass = p_1
- higher moments depend on n -point correlations

representation *separates*

GEOMETRY μ from
medium parameters in \mathcal{S}

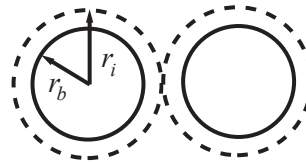
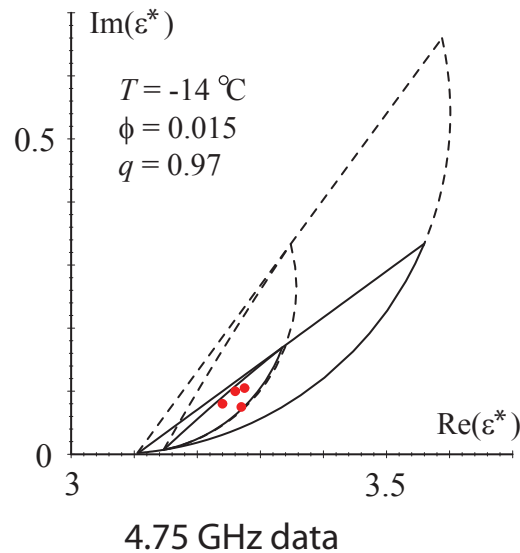
$$E = (s + \Gamma\chi)^{-1} e_k$$

$$\Gamma = \nabla(-\Delta)^{-1}\nabla.$$

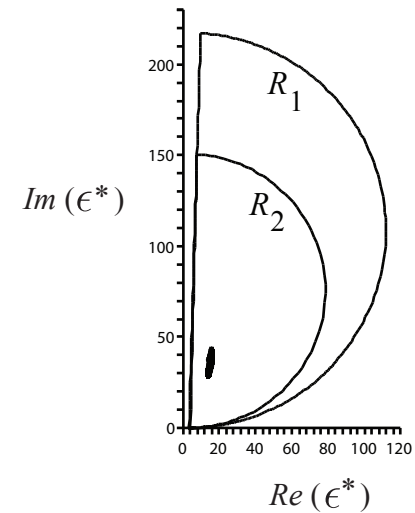
χ = indicator function
of medium 1

forward and inverse bounds for sea ice

matrix particle bounds



Golden 1997



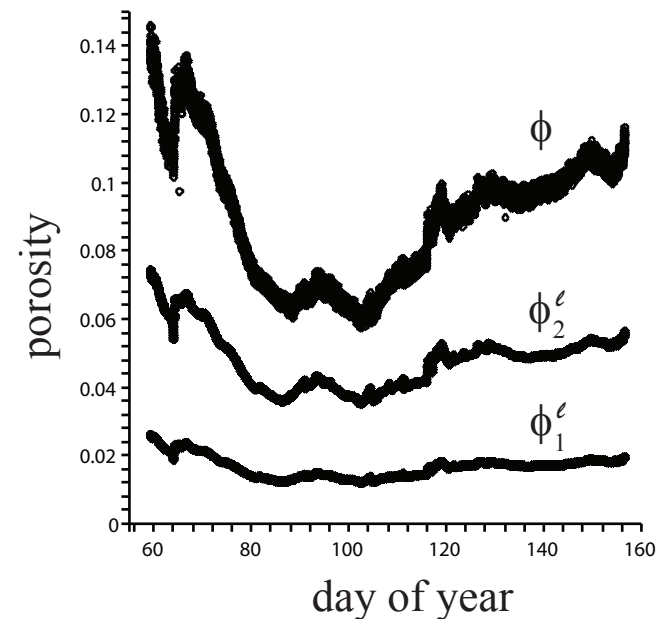
50 MHz capacitance probe data taken near Barrow, AK

inverse bounds and microstructural recovery

Gully, Backstrom, Eicken, Golden, Physica B, 2007

polycrystalline bounds

Gully, Lin, Cherkaev, Golden, 2012

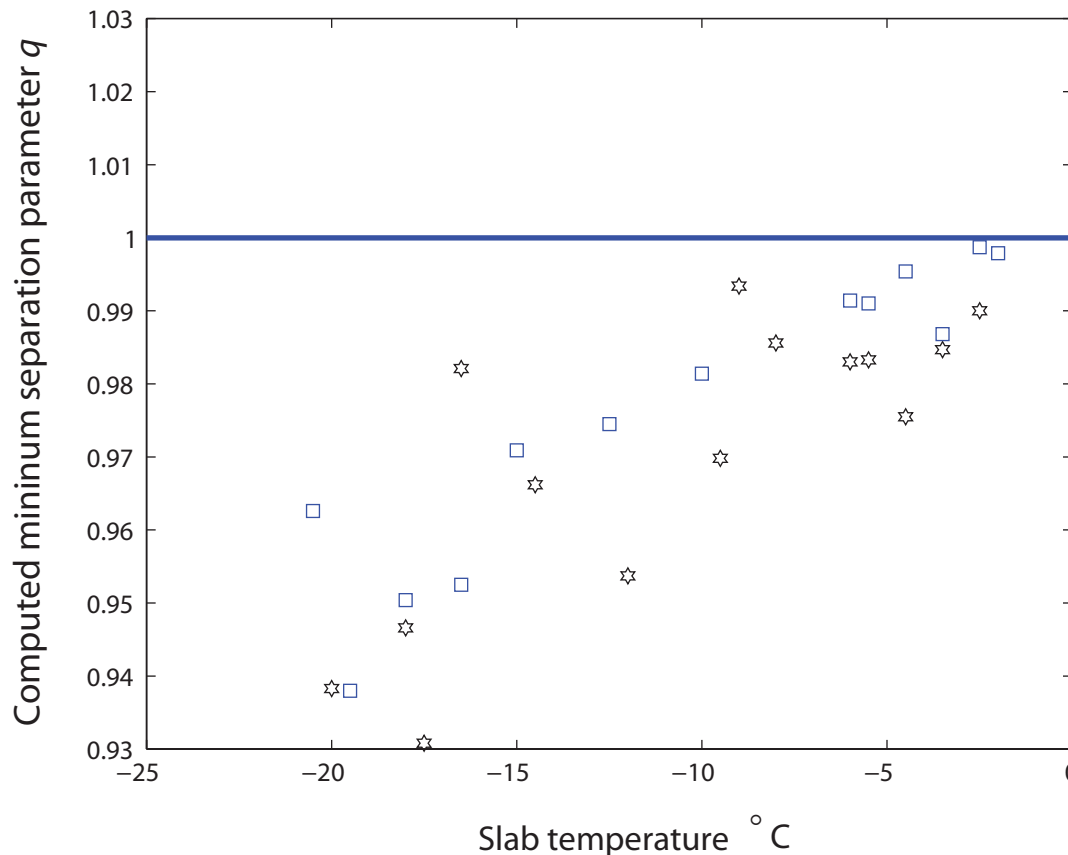


Recovery of inclusion separations in strongly heterogeneous composites from effective property measurements

Chris Orum, Elena Cherkaev, Ken Golden, Proc. Roy. Soc. A, 2012

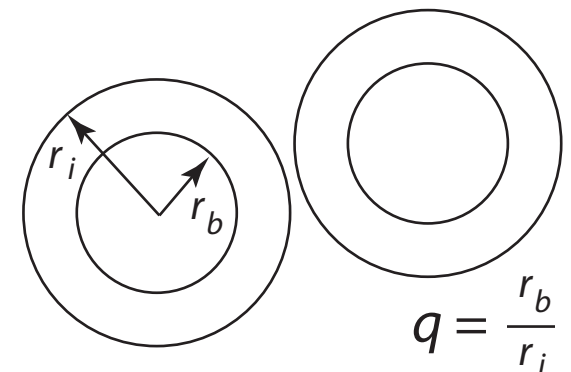
matrix particle composites (O. Bruno, 1991)

reduced spectral inversion -- construct algebraic curves which bound admissible region in (p,q) -space, q = separation parameter < 1

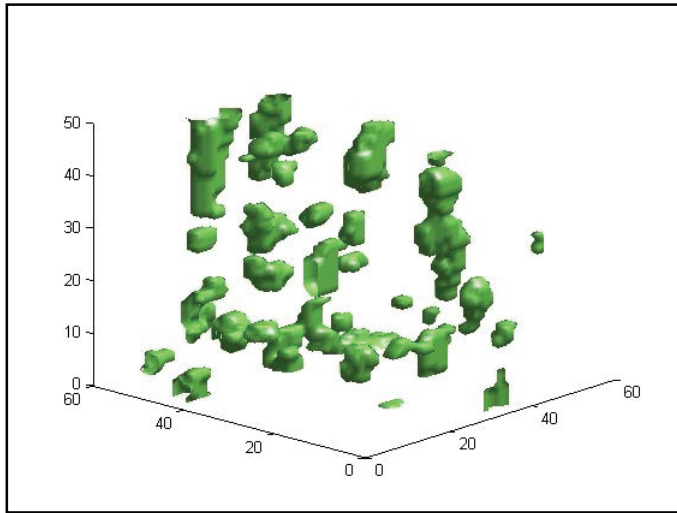


***rigorous inverse bound
on spectral gap***

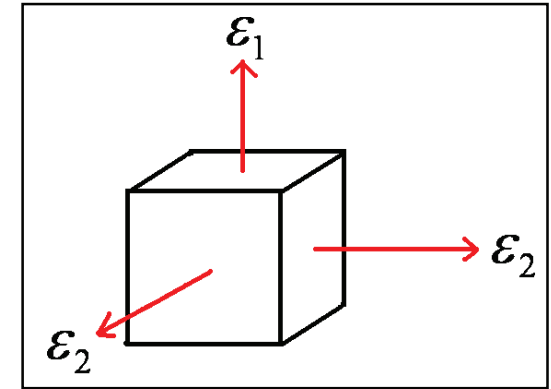
***inversion for brine inclusion
separations in sea ice from
measurements of effective
complex permittivity***



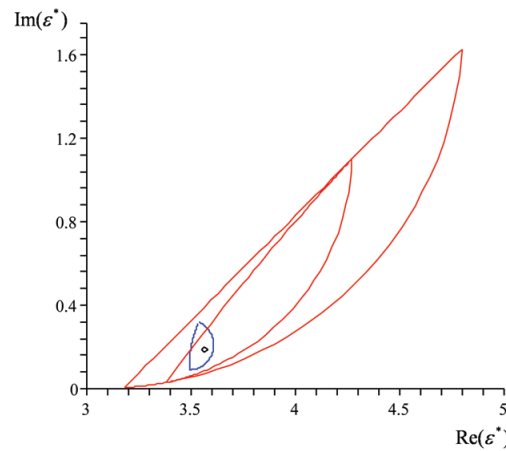
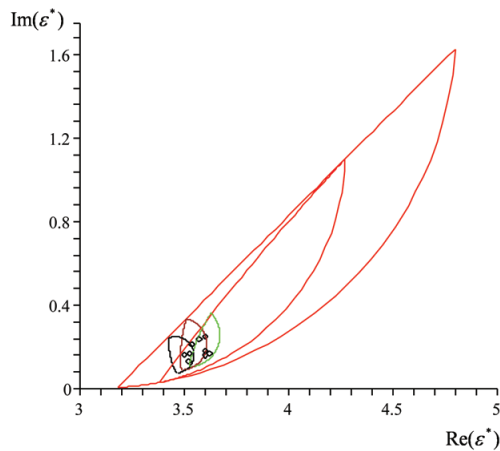
two scale homogenization for polycrystalline sea ice



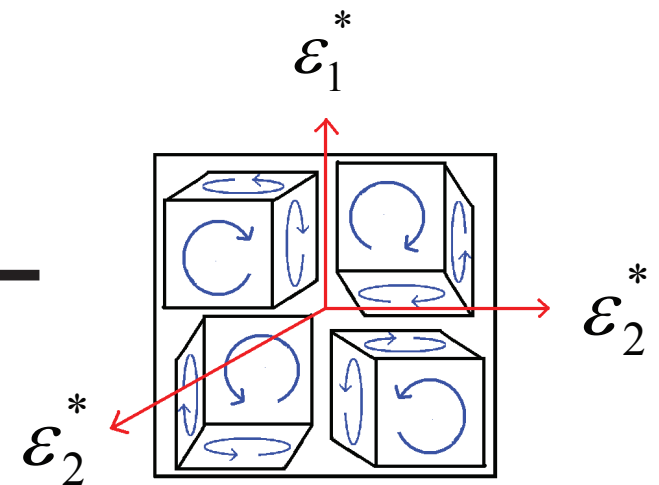
numerical homogenization
for single crystal



analytic continuation
for polycrystals



bounds



Gully, Lin, Cherkaev, Golden 2013

Spectral analysis of multiscale sea ice structures

homogenization for brine inclusions, melt ponds, and sea ice pack

**how to upscale information on “microstructure”
into effective behavior for larger scales**

numerical computation of spectral measure μ

N. B. Murphy, C. Hohenegger, C. S. Sampson, B. Alali, K. Steffen, D. K. Perovich, H. Eicken, and K. M. Golden 2012

direct calculation of spectral measure

1. Discretization of composite microstructure gives lattice of 1's and 0's (random resistor network).
2. The fundamental operator $\Gamma\chi$ becomes a random matrix depending only on the composite geometry.
3. Compute the eigenvalues λ_i and eigenvectors of $\Gamma\chi$ with $(\text{length})^2 = \alpha_i$

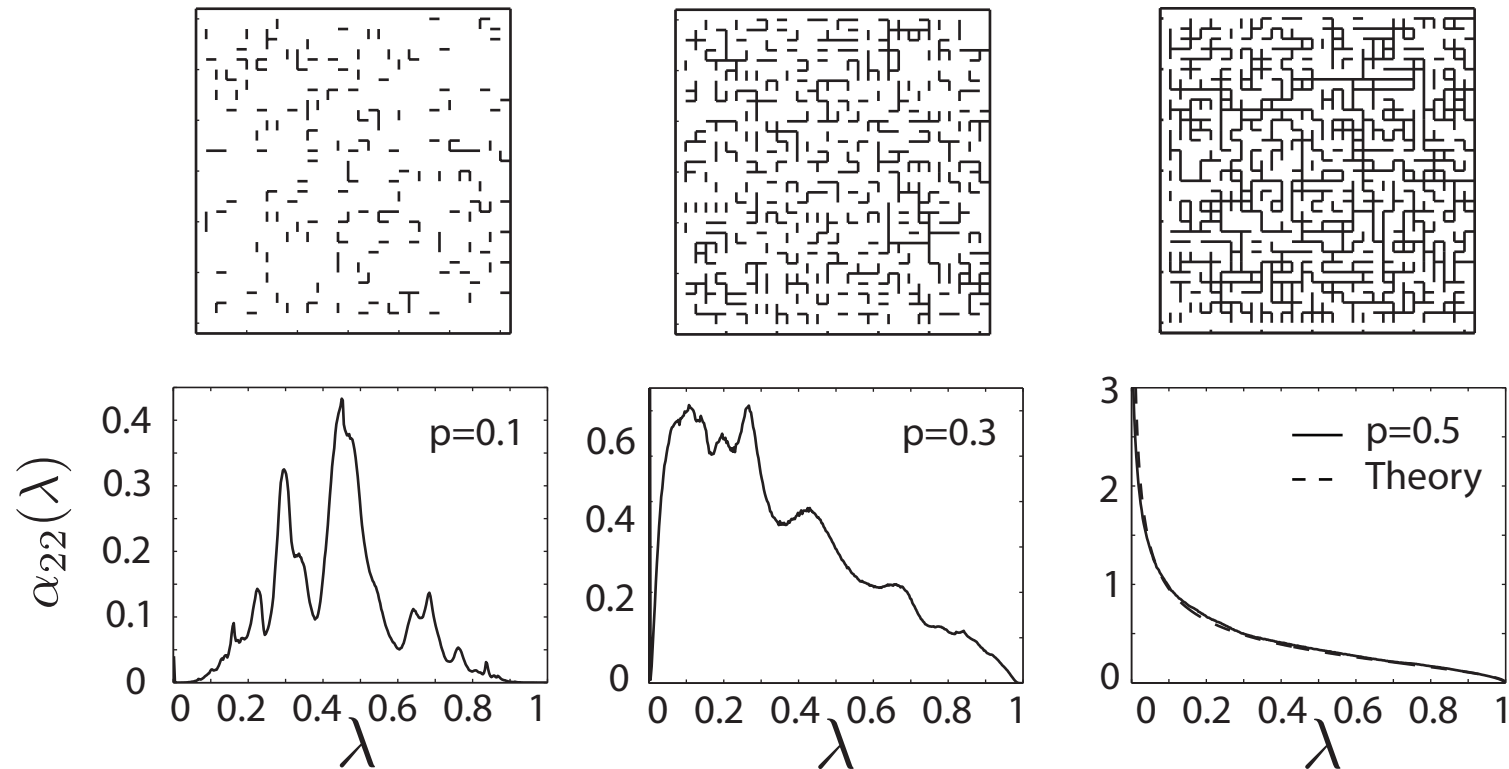
$$\mu(\lambda) = \sum_i \alpha_i \delta(\lambda - \lambda_i)$$



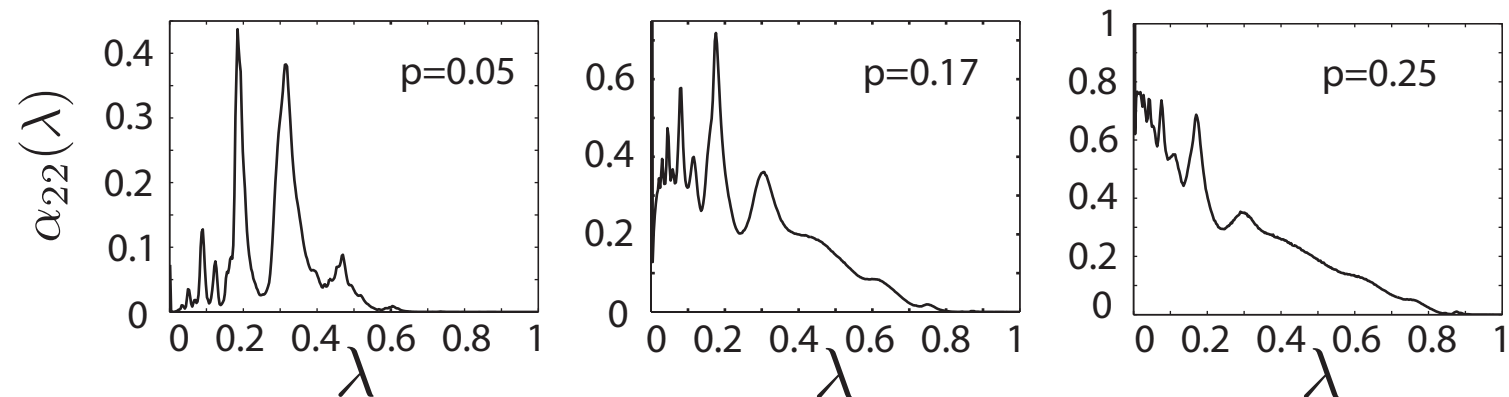
Dirac point measure (Dirac delta)

The Spectral Measures for Random Resistor Networks

2-D



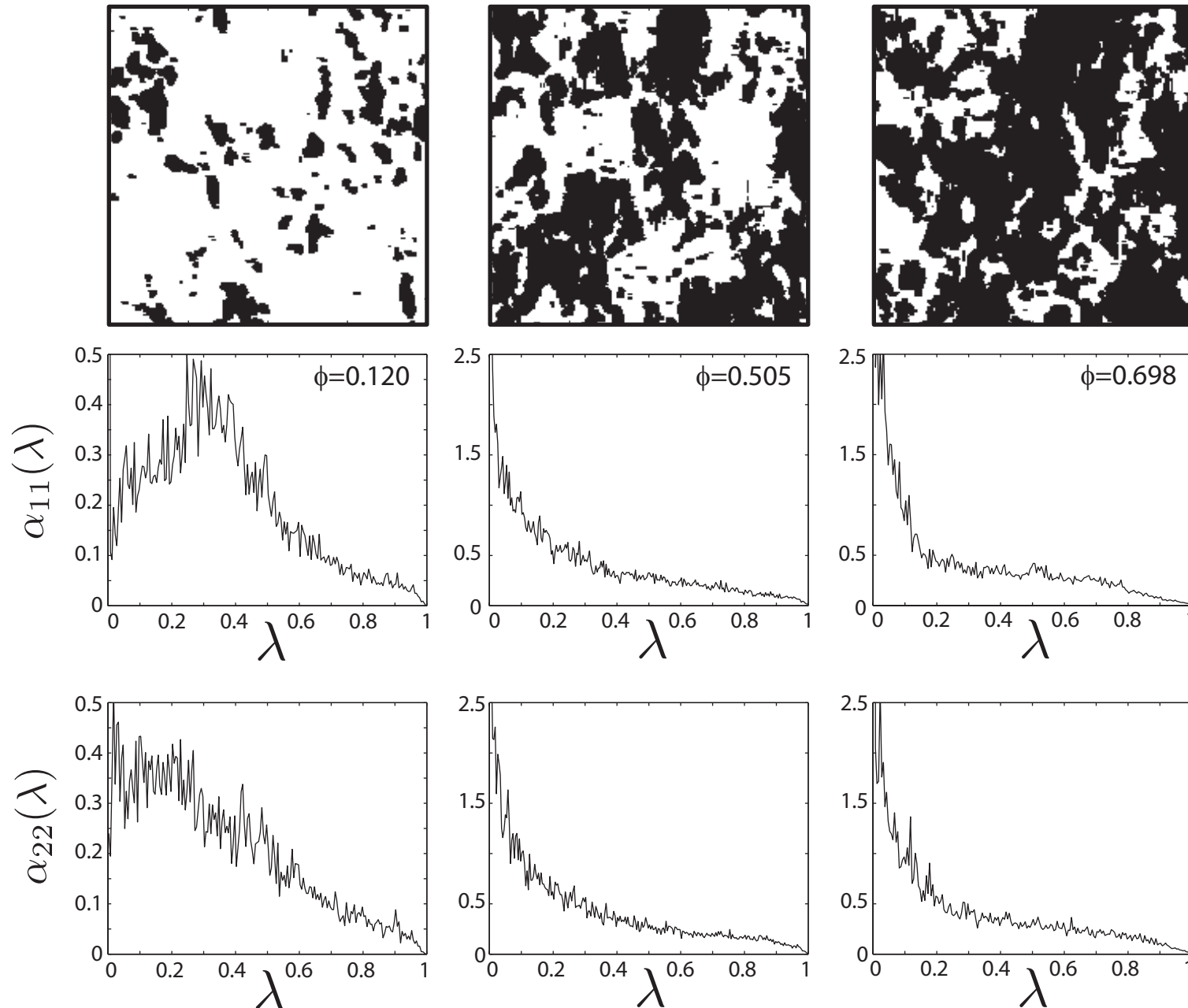
3-D



spectral gaps collapse at the percolation transitions

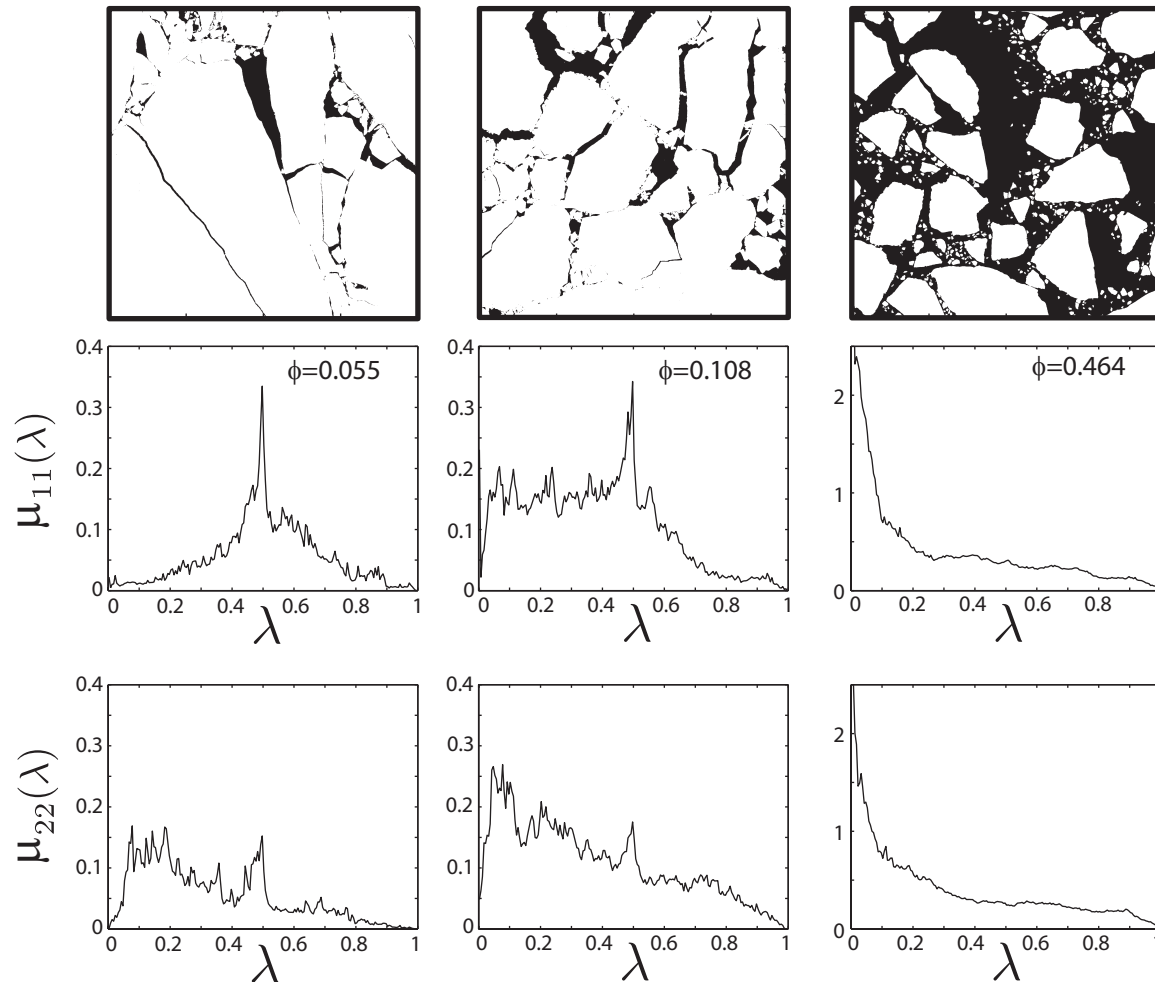
Murphy and Golden, J. Math. Phys. (2012)

Spectral Measures for Sea Ice Structures: Brine Inclusions



spectral measures provide a path toward rigorously incorporating
“composite microstructure” into calculations of effective behavior on larger scales

spectral measures for the Arctic sea ice pack



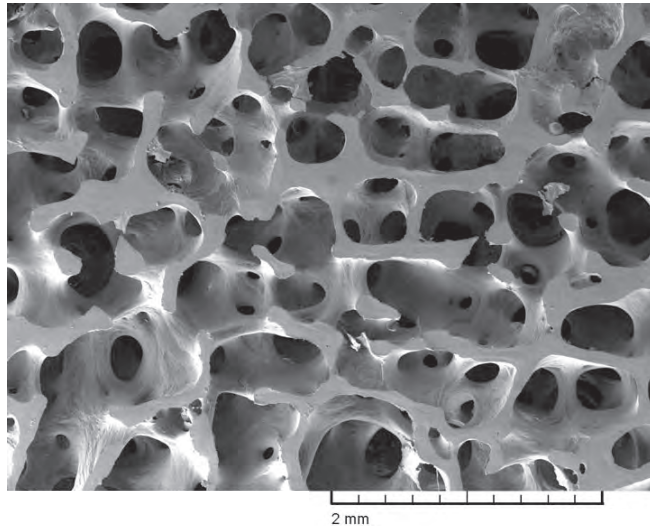
area under curve = ϕ = open water fraction

spectral gap closes as ocean phase becomes connected

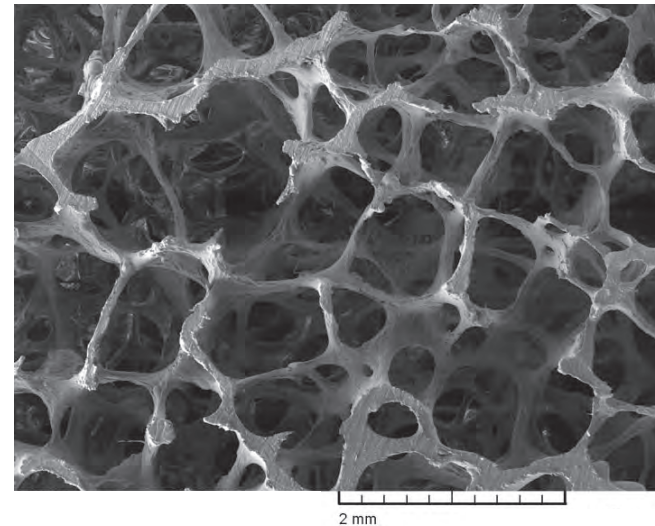
spectral characterization of porous microstructures in bone

Golden, Murphy, Cherkaev, J. Biomechanics 2011

(a) young healthy trabecular bone

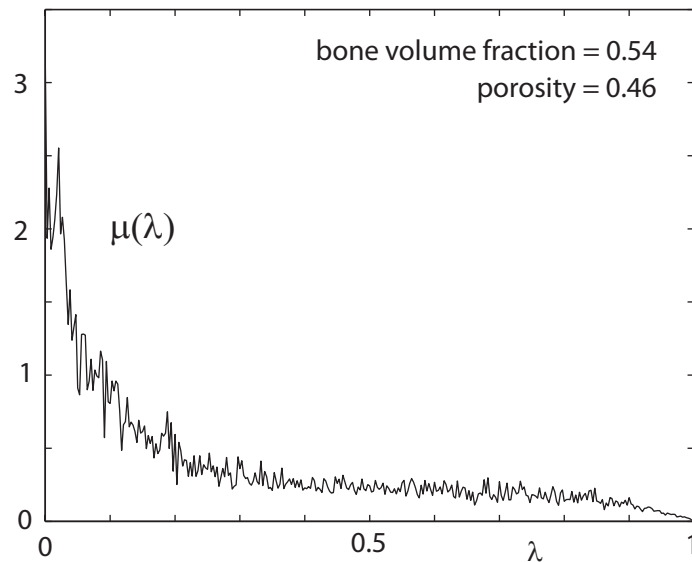


(b) old osteoporotic trabecular bone

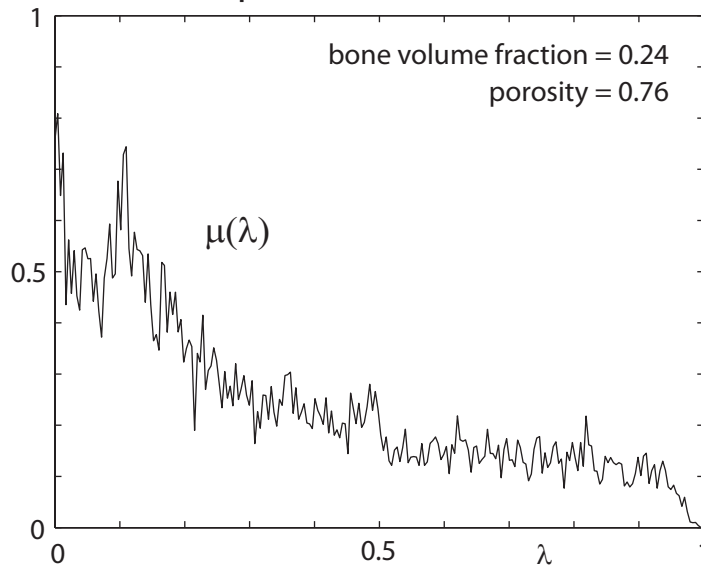


P. Hansma

(c) spectral measure - young

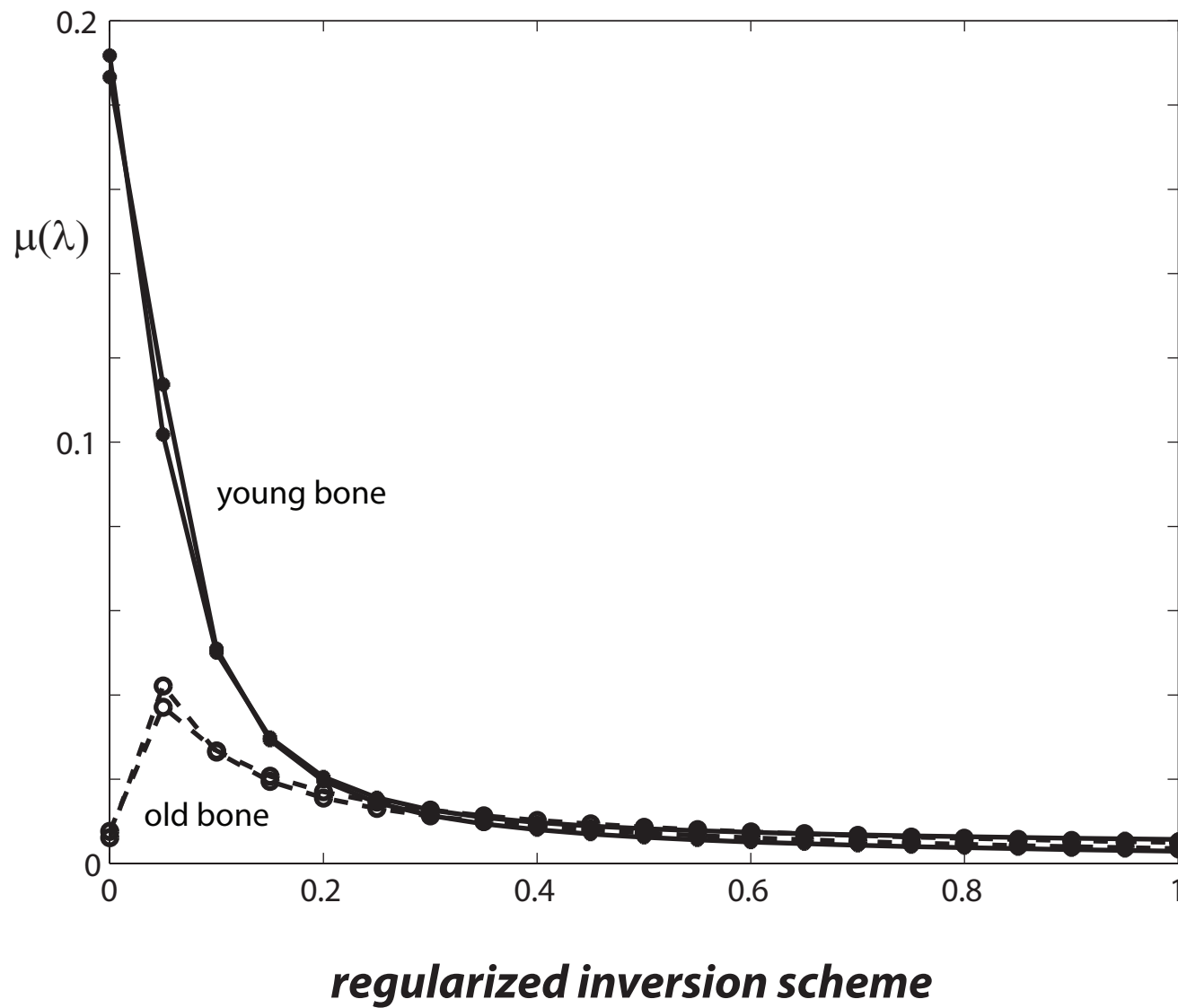


(d) spectral measure - old



the math doesn't care if it's sea ice or bone!

reconstruction of spectral measures from simulated complex permittivity data



Random Matrix Theory Characterization of Phase Transitions

$$\chi_2 \Gamma \chi_2 \} \longleftarrow \text{Real Symmetric Random Matrix}$$

\uparrow *Random* Diagonal Projection Matrix \uparrow *Non-Random* Projection Matrix

- The elements of a random matrix are determined by a probability law.
- Wigner (1951) and Dyson (1953) first used random matrix theory (RMT) to describe quantized energy levels of heavy atomic nuclei.
- RMT has since been used to characterize: phase transitions in disordered mesoscopic conductors, quantum chaos, neural networks, random graphs, etc.
- *In composites*, connectedness transitions can be characterized by transitions in the short and long range correlations of eigenvalues of the matrix $\chi_2 \Gamma \chi_2$.

- The eigenvectors may be integrated out, and *the probability distribution is exactly that of the canonical ensemble of 2-D positive charges on a line!*

$$P_N = Z_N^{-1} \exp(-\mathcal{H}_N), \quad \mathcal{H}_N = \sum_{i=1}^N V(\lambda_i) - \sum_{i>j=1}^N \ln |\lambda_i - \lambda_j|$$

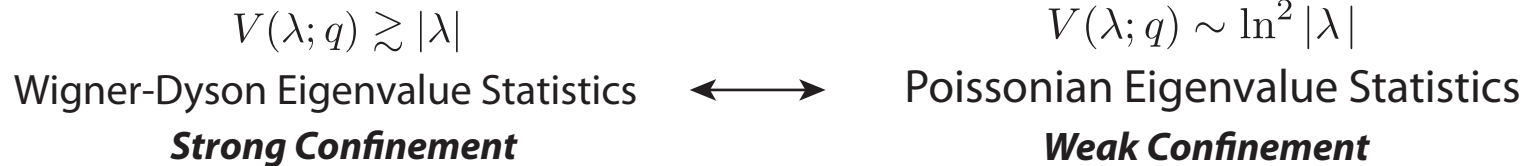
Energy
Hamiltonian
of Eigenvalues

Confining
Potential

Logarithmic Repulsion
of Eigenvalues

- The mean eigenvalue density ρ depends on the form of V , although, the *fluctuations* about the mean density *are universal*.
- In order to observe the universal fluctuations of eigenvalues about the mean density, they are **unfolded** to have **unit mean spacing**.

Phase Transitions in Random Matrix Theory



- **Phase transitions** are modeled by allowing the potential V to vary as a function of a **disorder parameter** q .

- When $V(\lambda; q) \gtrsim |\lambda|$ for $|\lambda| \gg 1$, highly correlated **Wigner-Dyson** (WD) **eigenvalue statistics** give rise to the phenomenon of **level repulsion**:

$$P(z) \approx \frac{\pi z}{2} \exp(-\pi z^2/4) \quad (\text{The Wigner Surmise})$$

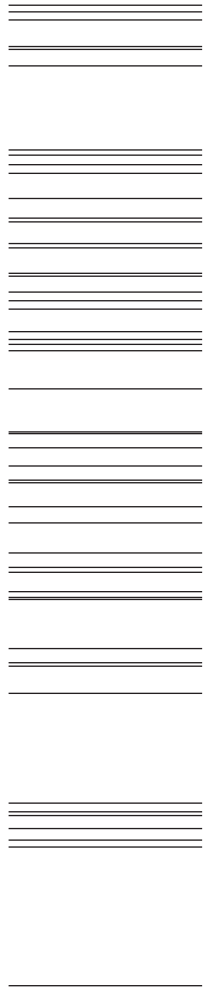
- When $V(\lambda; q) \sim \ln^2 |\lambda|$ for $|\lambda| \gg 1$, the eigenvalues are weakly correlated, giving rise to **Poissonian eigenvalue statistics**.

Transitions in Eigenvalue Correlations

$$P(z) = \exp(-z)$$

Eigenvalue Spacing Distribution

**Poisson
Spectra**

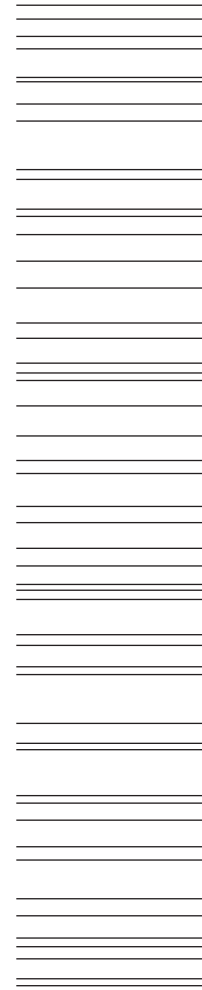


Uncorrelated

$$P(z) \approx \frac{\pi z}{2} \exp(-\pi z^2/4)$$

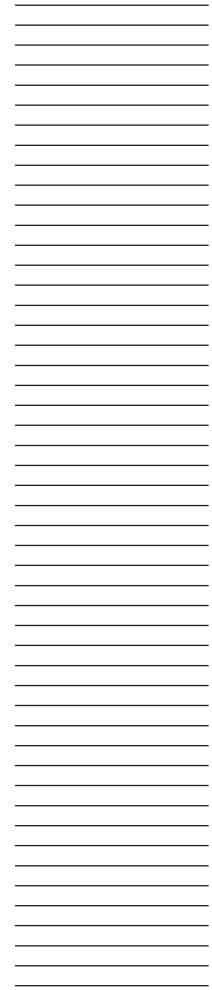
Eigenvalue Spacing Distribution

**WD
Spectra**



**Highly
Correlated**

**Picket
Fence**



**Completely
Correlated**

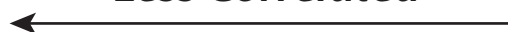
Phase Transition



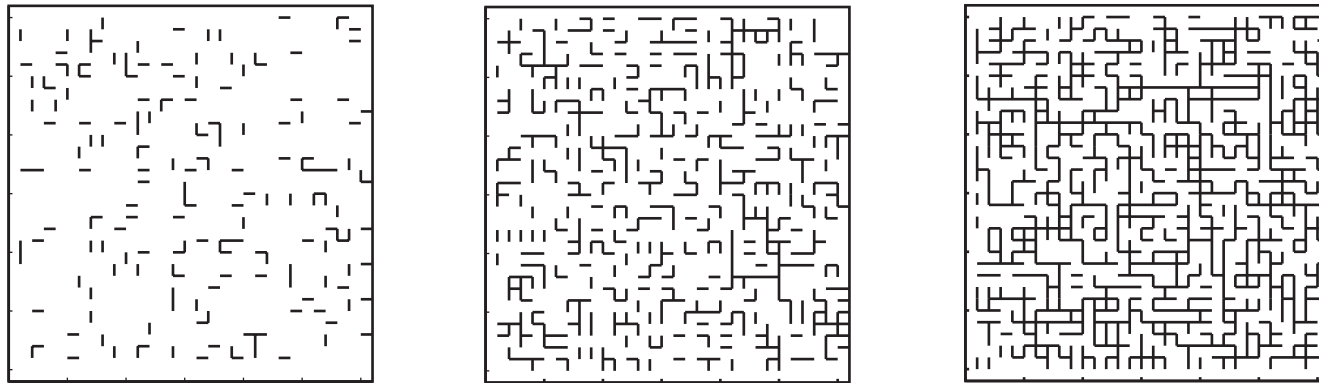
Less Level Repulsion



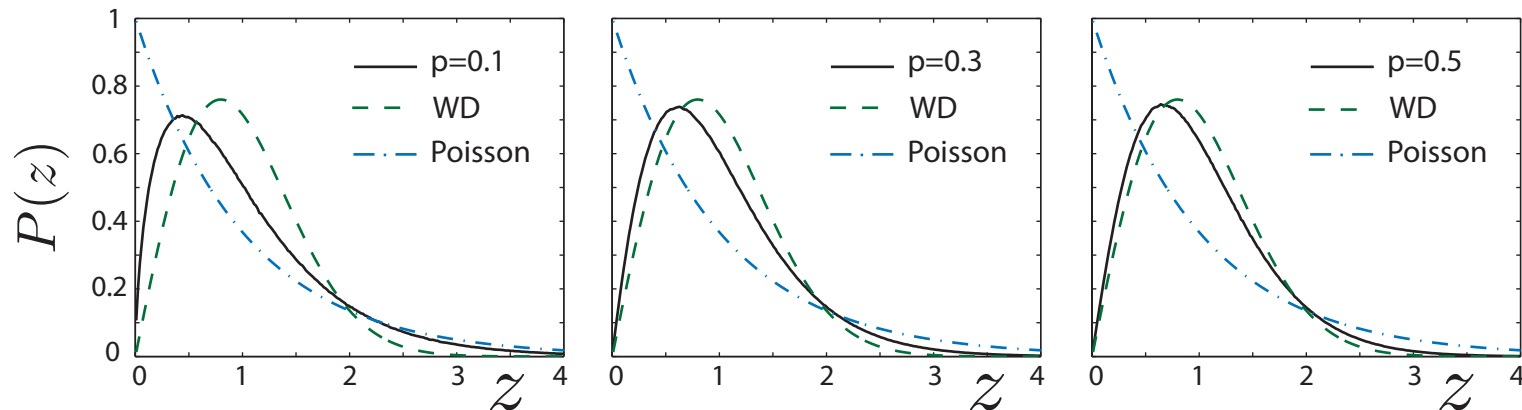
Less Correlated



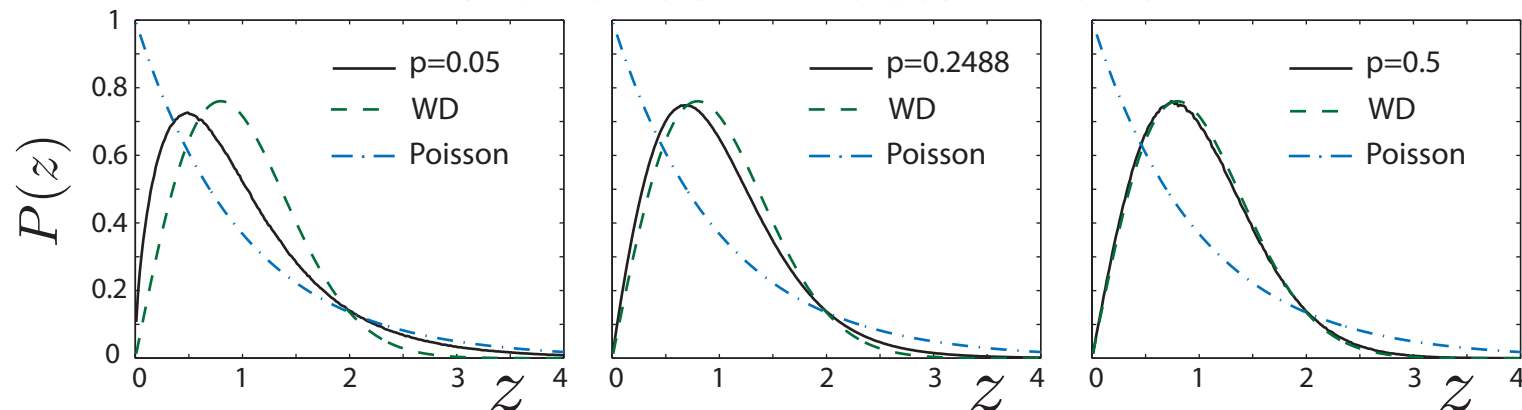
Unfolded Eigenvalue Spacing Distribution



2-d Random Resistor Network

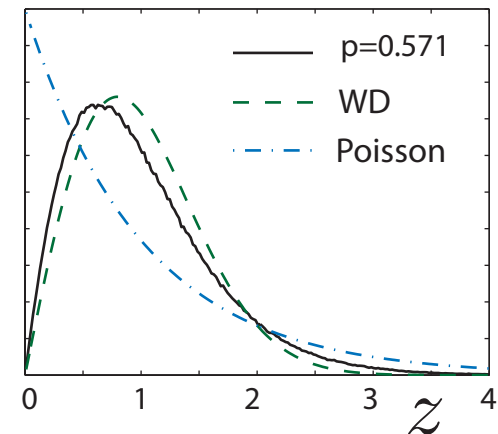
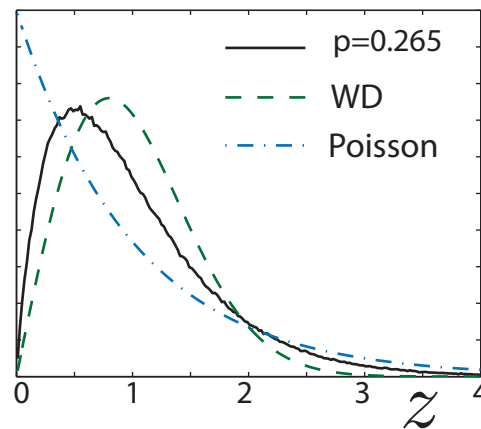
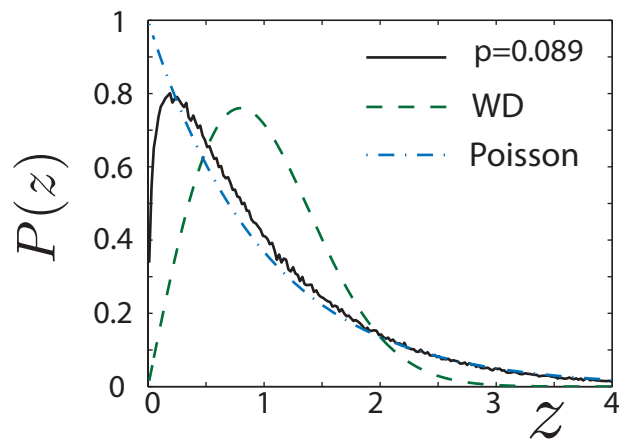
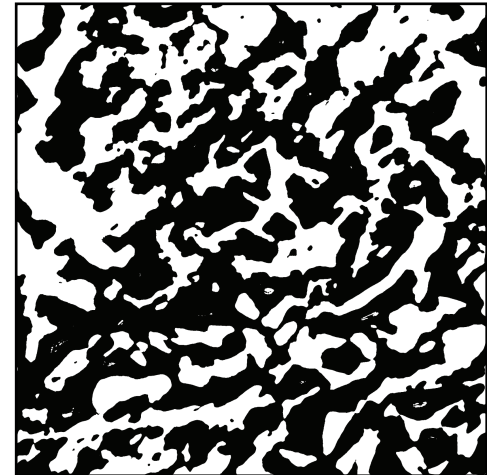
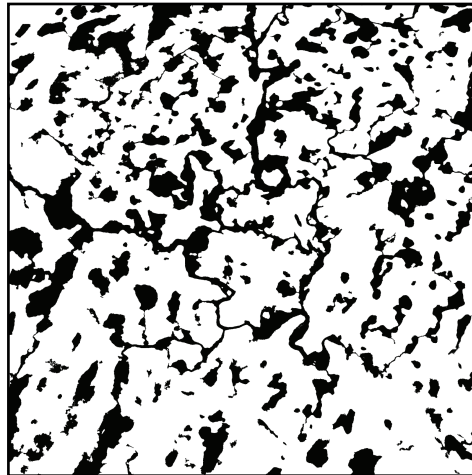
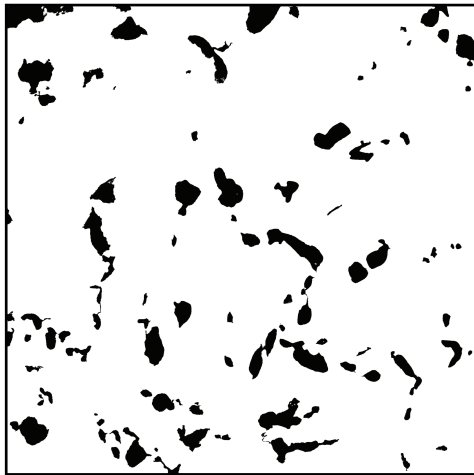


3-d Random Resistor Network



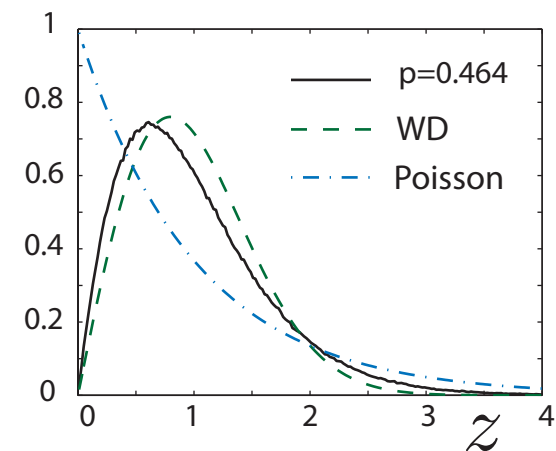
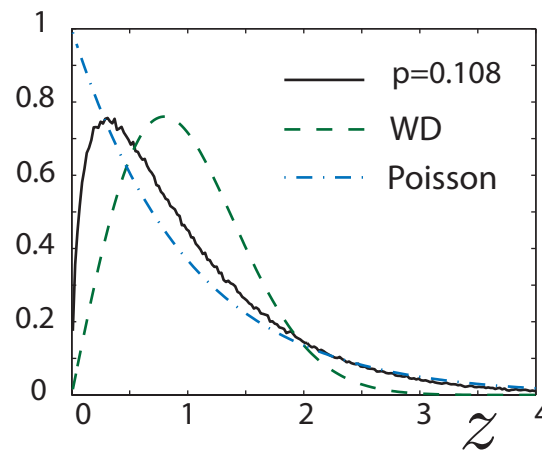
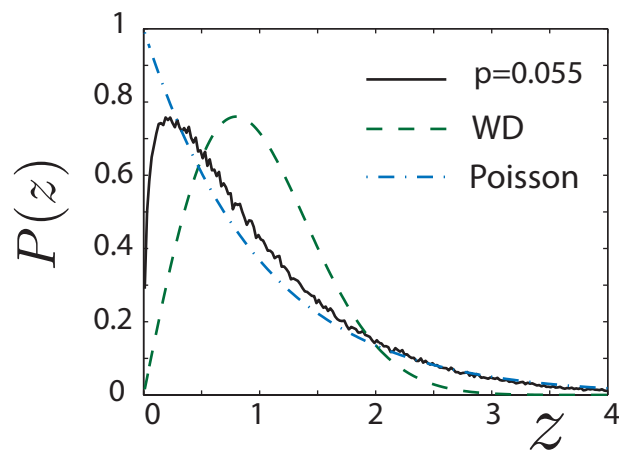
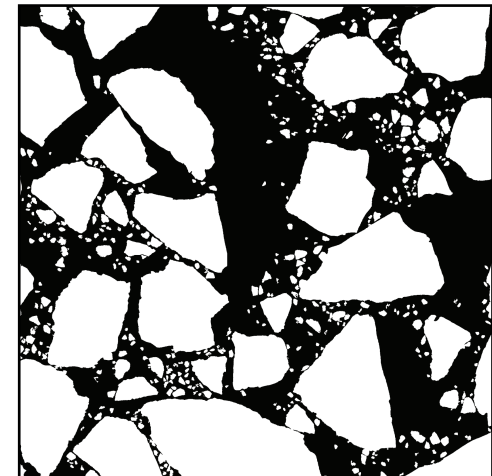
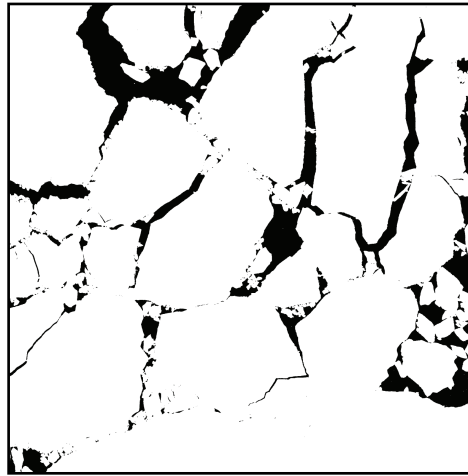
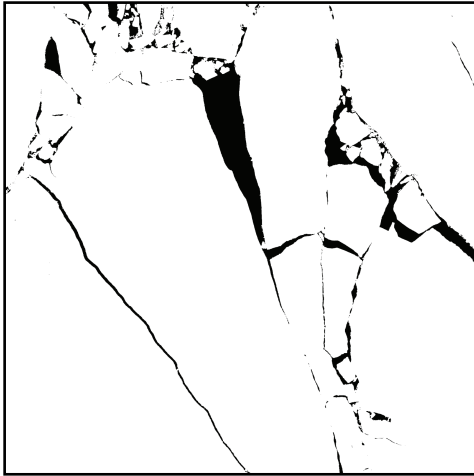
Unfolded Eigenvalue Spacing Distribution

ARCTIC MELT PONDS



Unfolded Eigenvalue Spacing Distribution

ARCTIC SEA ICE PACK



advection enhanced diffusion

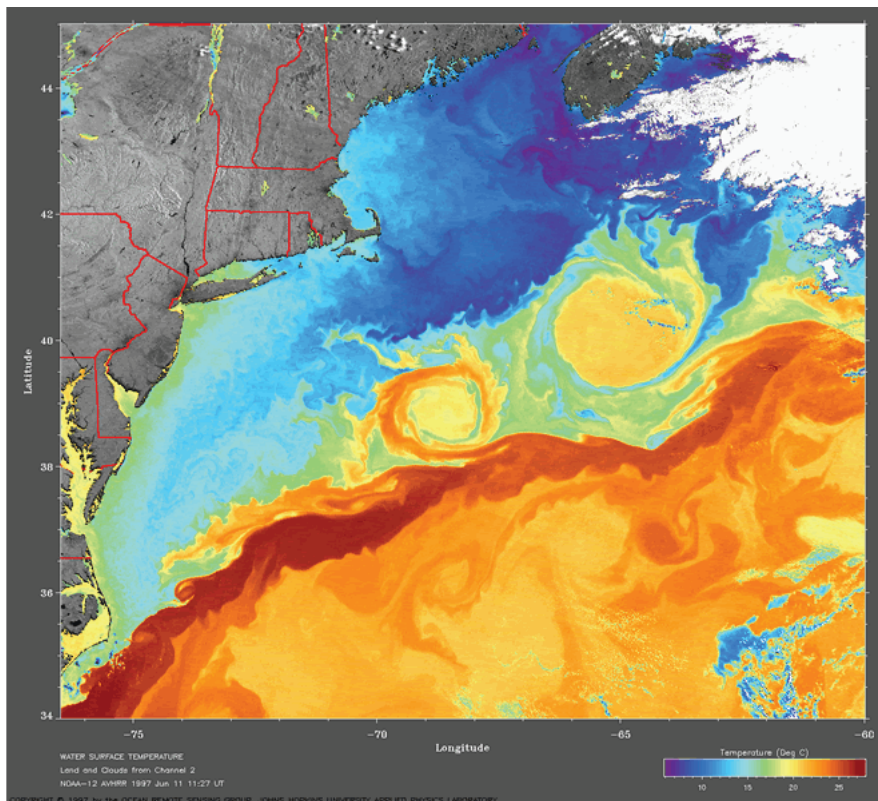
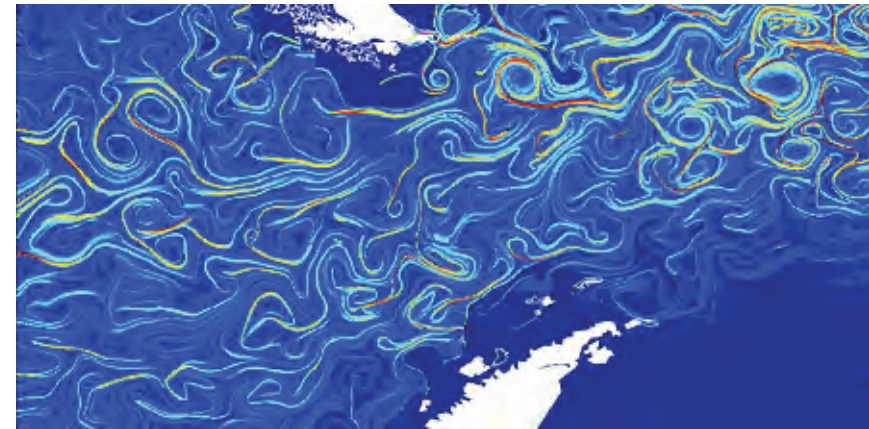
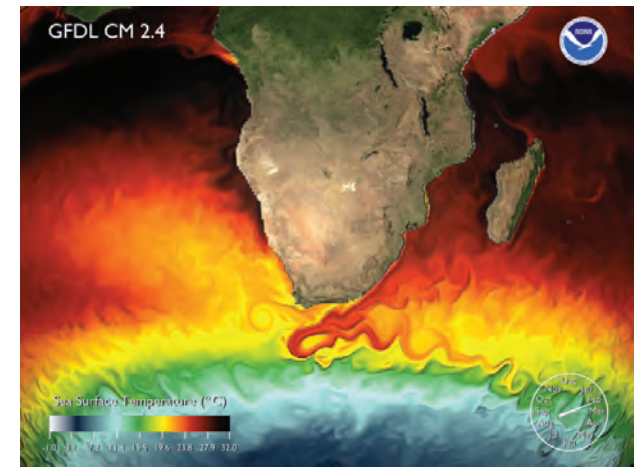
effective diffusivity

tracers, buoys diffusing in ocean eddies

pollutants

enhanced heat and salt transport

enhanced sea ice thermal conductivity



advection diffusion equation with a velocity field \vec{u}

$$\frac{\partial T}{\partial t} + \vec{u} \cdot \vec{\nabla} T = \kappa_0 \Delta T$$

$$\vec{\nabla} \cdot \vec{u} = 0$$

homogenize

$$\frac{\partial \bar{T}}{\partial t} = \kappa^* \Delta \bar{T}$$

κ^* effective diffusivity

Stieltjes integral for κ^* with spectral measure

Avellaneda and Majda, PRL 89, CMP 91

composites

$$\frac{\epsilon^*}{\epsilon_2} = 1 - \int_0^1 \frac{d\mu(\lambda)}{s - \lambda}$$

$$s = \frac{1}{1 - \epsilon_1 / \epsilon_2}$$

μ spectral measure of $\chi \Gamma \chi$

advection diffusion

$$\frac{\kappa^*}{\kappa_0} = 1 + \xi^2 \int_0^\infty \frac{d\phi(\tau)}{1 + \xi^2 \tau^2}$$

ξ = Péclet number

ϕ spectral measure of $i\Gamma \mathbf{H} \Gamma$

$\vec{u} = \kappa_0 \xi \vec{\nabla} \cdot \mathbf{H}$, \mathbf{H} antisymmetric vector potential

Spectral Calculation of Effective Parameters

composites

Real Symmetric Random Matrix

$$\chi \Gamma \chi = \mathbf{U} \Lambda \mathbf{U}^T$$

$$\frac{\epsilon^*}{\epsilon_2} = 1 - \int_0^1 \frac{d\mu(\lambda)}{s - \lambda}$$

$$\int_0^1 \frac{d\mu(\lambda)}{s - \lambda} = \sum_j \frac{\mu_j}{s - \lambda_j}$$

$$\mu_j = \langle (\vec{u}_j^T \vec{e}_k)^2 \rangle$$

λ_j eigenvalues of the **matrix** $\chi \Gamma \chi$
with **real** eigenvectors \vec{u}_j

advection diffusion

Hermitian Random Matrix

$$\mathbf{i} \Gamma \mathbf{H} \Gamma = \mathbf{V}^\dagger \mathbf{T} \mathbf{V}$$

$$\frac{\kappa^*}{\kappa_0} = 1 + \xi^2 \int_0^\infty \frac{d\phi(\tau)}{1 + \xi^2 \tau^2}$$

$$\int_0^\infty \frac{d\phi(\tau)}{1 + \xi^2 \tau^2} = \sum_j \frac{\phi_j}{1 + \xi^2 \tau_j^2}$$

$$\phi_j = \langle |\vec{v}_j^\dagger \Gamma \mathbf{H} \vec{e}_k|^2 \rangle$$

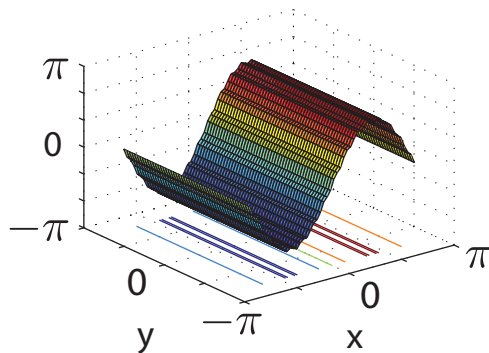
τ_j eigenvalues of the **matrix** $\mathbf{i} \Gamma \mathbf{H} \Gamma$
with **complex** eigenvectors \vec{v}_j

The projective nature of χ and Γ leads to an efficient way of calculating the spectral measures, which is also numerically stable and reduces roundoff error.

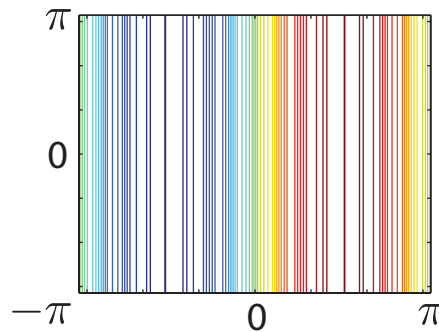
spectral measures for sample flows

Shear Flow: $H(x, y) = \sin x + (0.5 + \eta) \sin(15x)/15, \quad \eta \sim U(-0.1, 0.1)$

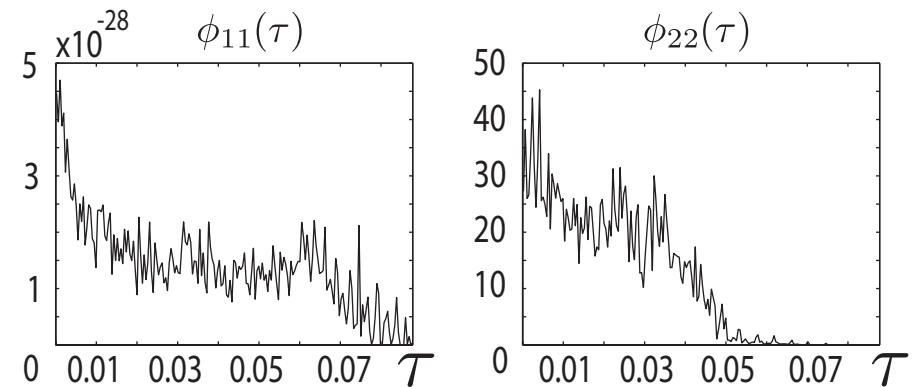
stream function



streamlines

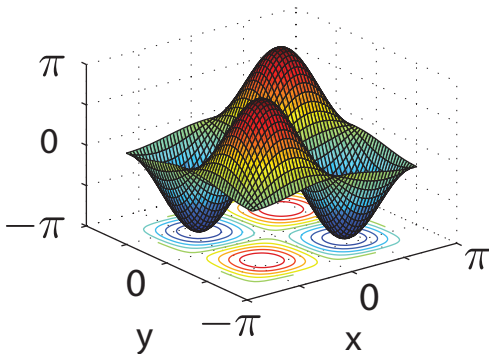


spectral functions

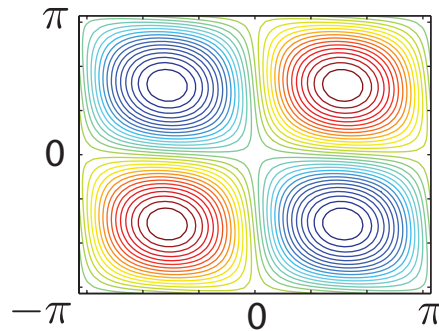


Modified Cat's Eye Flow: $H(x, y) = \sin x \sin y + \eta \cos x \cos y, \quad \eta \sim U(-0.1, 0.1)$

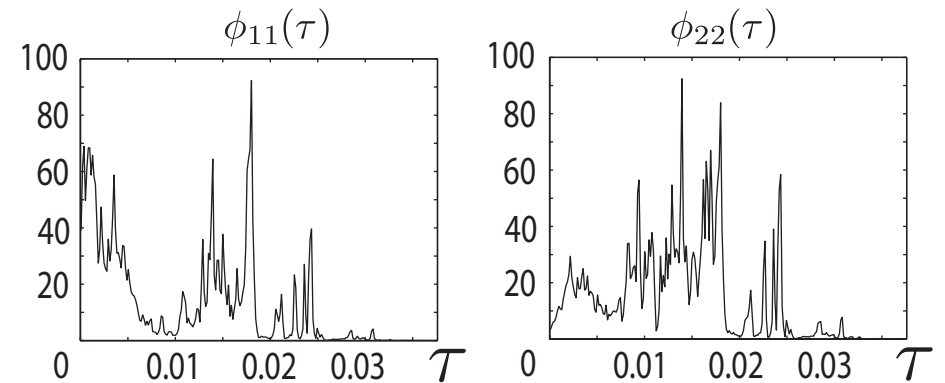
stream function



streamlines



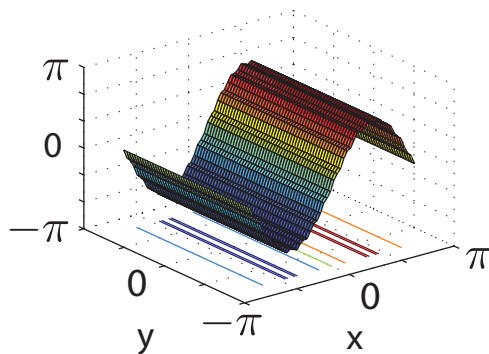
spectral functions



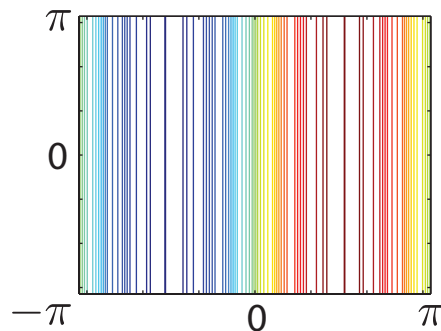
effective diffusivities for sample flows

Shear Flow: $H(x, y) = \sin x + (0.5 + \eta) \sin(15x)/15$, $\eta \sim U(-0.1, 0.1)$

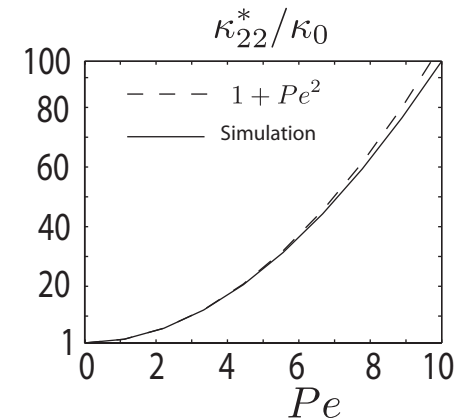
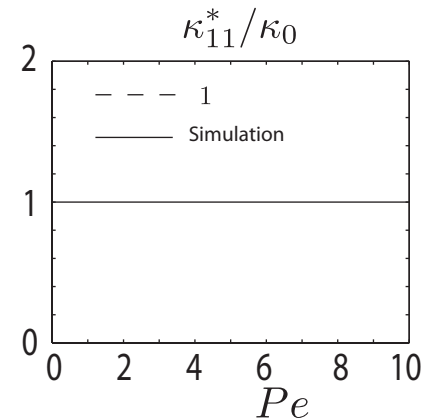
stream function



streamlines

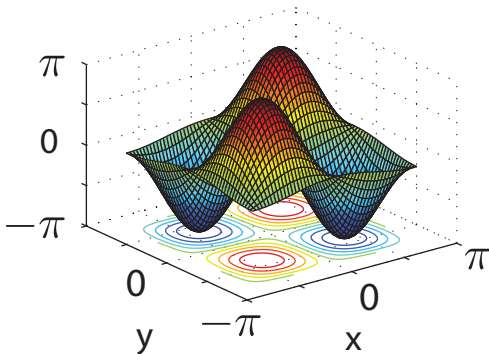


effective diffusivities

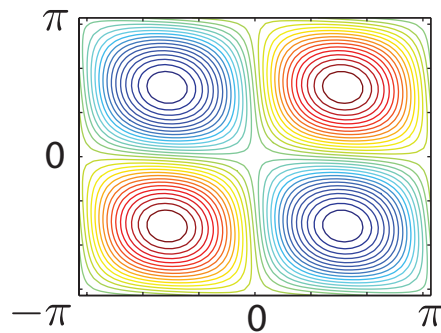


Modified Cat's Eye Flow: $H(x, y) = \sin x \sin y + \eta \cos x \cos y$, $\eta \sim U(-0.1, 0.1)$

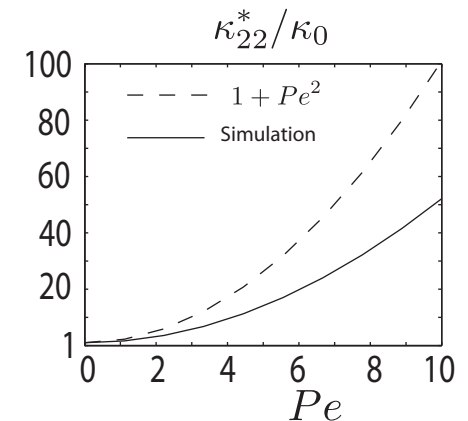
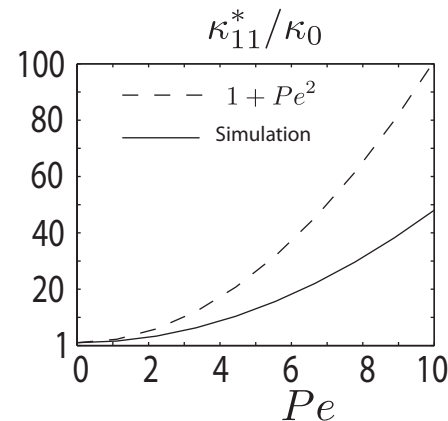
stream function



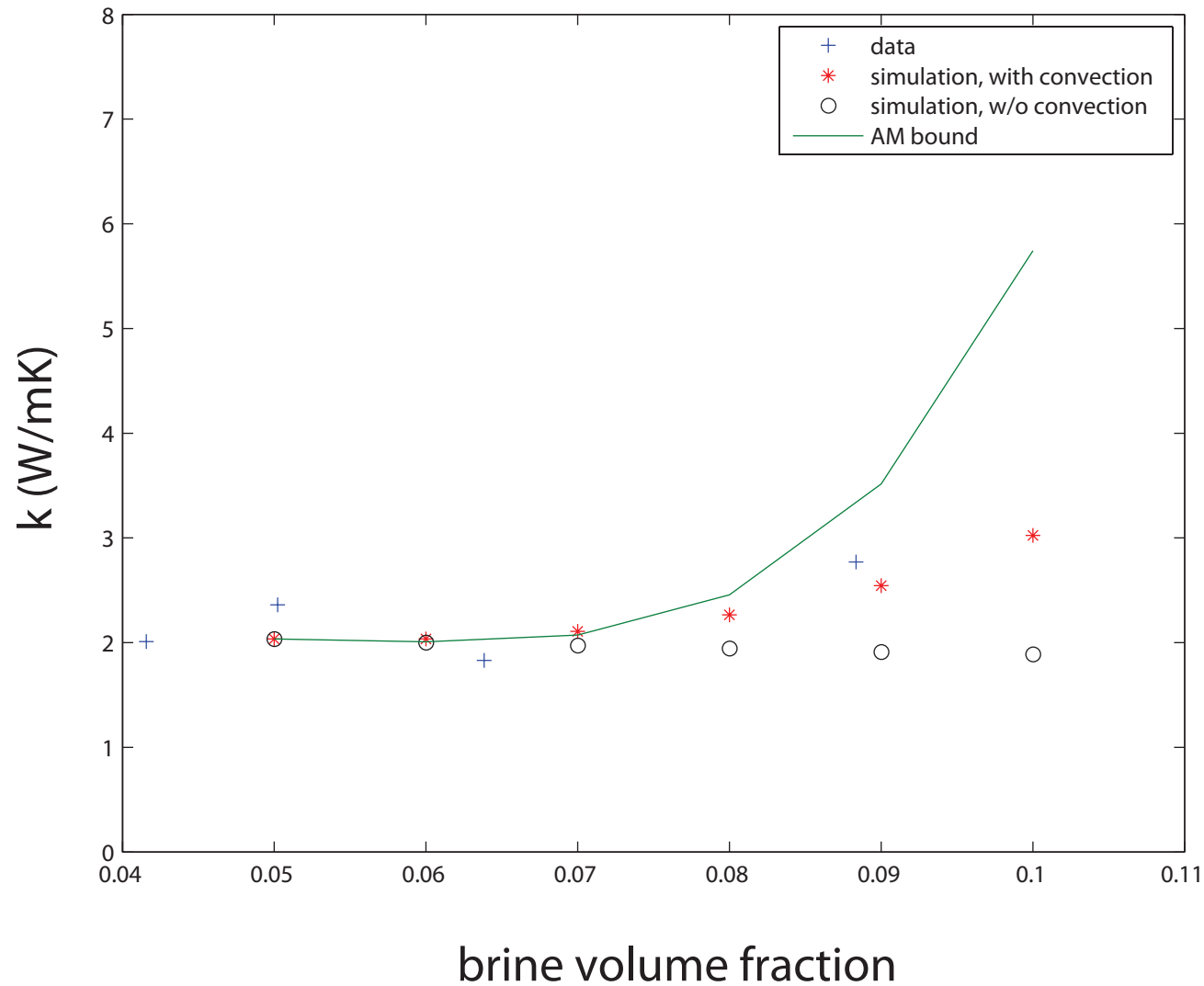
streamlines



effective diffusivities



convection enhanced thermal conductivity of sea ice for shear flow



Conclusions

1. Sea ice exhibits composite structure on many length scales.
2. Fluid flow through sea ice mediates many processes of importance to understanding climate change and the response of polar ecosystems.
3. Mathematical models of composite materials and statistical physics help unravel the complexities of sea ice structure and processes.
4. Homogenization theory and upscaling methods can provide a rigorous path to representing large scale effective behavior in coarse models.
5. Random matrix theory can help characterize transitions important for climate science and composite materials.

THANK YOU

National Science Foundation

Division of Mathematical Sciences

Arctic Natural Sciences

Office of Polar Programs

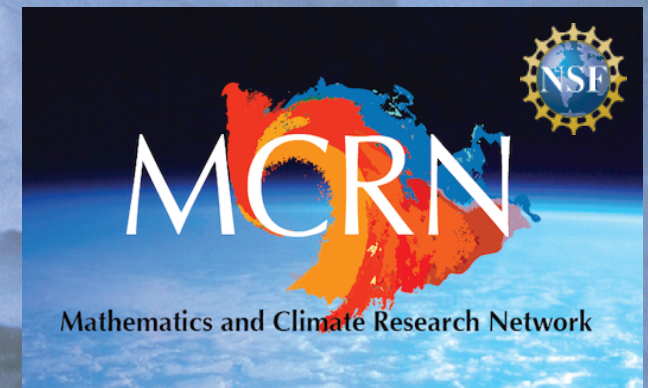
CMG Program

(Collaboration in Mathematical Geosciences)

Office of Naval Research

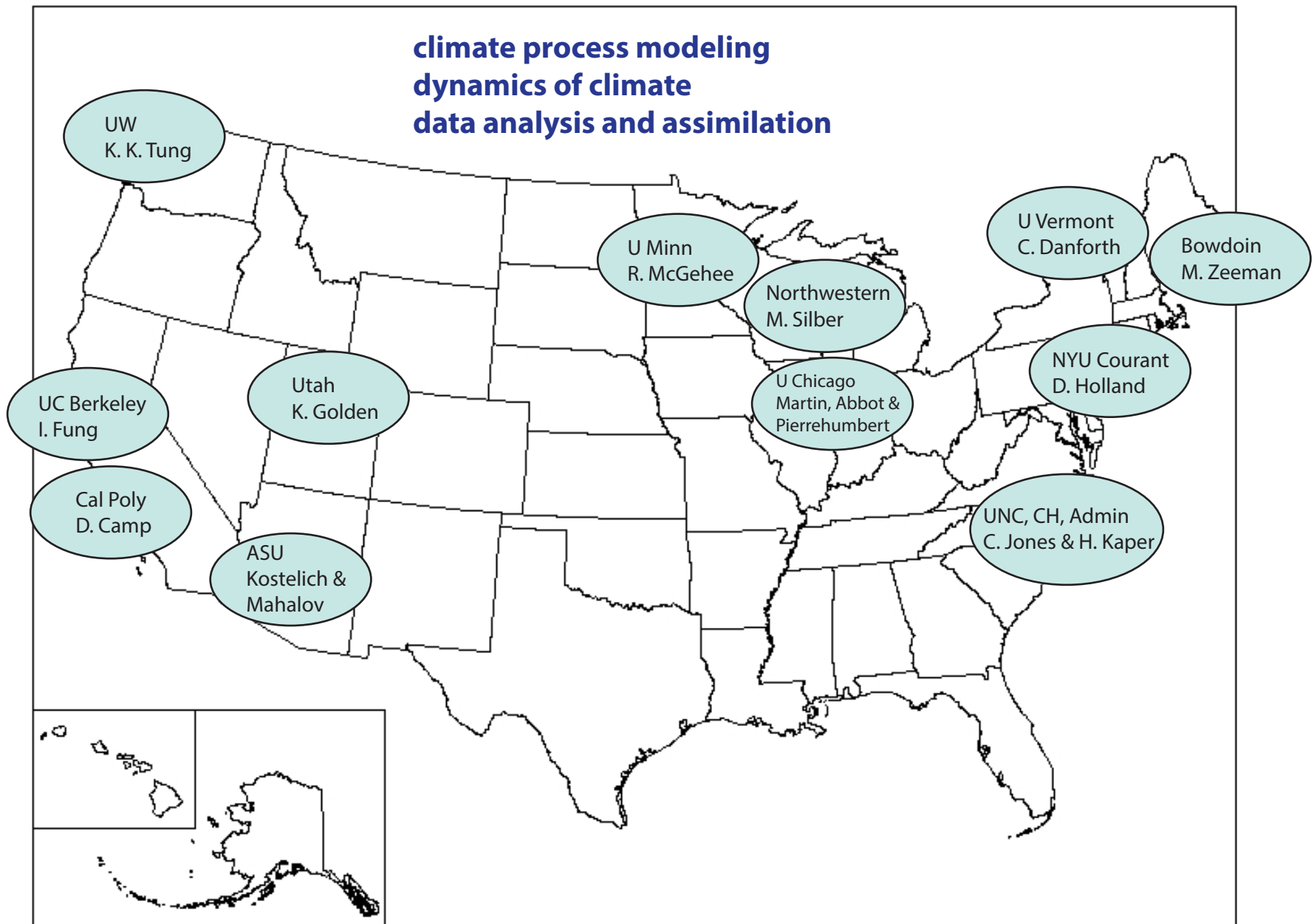
Applied Computational Analysis Program

Arctic and Global Prediction Program



Buchanan Bay, Antarctica Mertz Glacier Polynya Experiment July 1999

Mathematics and Climate Research Network (MCRN)



NSF DMS 2010-2015, Lorenz postdocs, grad, undergrad, polar expeditions

Jones, Golden, Kaper, Zeeman